



**HAL**  
open science

# Phase change dispersions: A literature review on their thermo-rheological performance for cooling applications

Poppy O'neill, Ludger Fischer, Rémi Revellin, Jocelyn Bonjour

## ► To cite this version:

Poppy O'neill, Ludger Fischer, Rémi Revellin, Jocelyn Bonjour. Phase change dispersions: A literature review on their thermo-rheological performance for cooling applications. *Applied Thermal Engineering*, 2021, 192, pp.116920. 10.1016/j.applthermaleng.2021.116920 . hal-03420499

**HAL Id: hal-03420499**

**<https://hal.science/hal-03420499v1>**

Submitted on 9 May 2023

**HAL** is a multi-disciplinary open access archive for the deposit and dissemination of scientific research documents, whether they are published or not. The documents may come from teaching and research institutions in France or abroad, or from public or private research centers.

L'archive ouverte pluridisciplinaire **HAL**, est destinée au dépôt et à la diffusion de documents scientifiques de niveau recherche, publiés ou non, émanant des établissements d'enseignement et de recherche français ou étrangers, des laboratoires publics ou privés.



Distributed under a Creative Commons Attribution - NonCommercial 4.0 International License

# Phase change dispersions: a literature review on their thermo-rheological performance for cooling applications

Poppy O'Neill<sup>a,b</sup>, Ludger Fischer<sup>b</sup>, Rémi Revellin<sup>a</sup> and Jocelyn Bonjour<sup>a,\*</sup>

<sup>a</sup>Univ Lyon, INSA Lyon, CNRS, CETHIL, UMR5008, 69621 Villeurbanne, France

<sup>b</sup>Lucerne University of Applied Sciences and Arts, 6048, Horw, Switzerland

## ARTICLE INFO

### Keywords:

Heat transfer fluid  
Phase change emulsion  
Phase change material  
Convective heat transfer

## ABSTRACT


Phase change dispersions are two-phase fluids that consist of a phase change material dispersed in a continuous phase and stabilised with the aid of surfactants. Due to the high thermal storage capacity, on accounts of the latent heat of phase change of the dispersed phase change material, phase change dispersions present as prospective heat transfer fluids in cooling applications. However, to implement phase change dispersions into cooling systems, for the design of heat exchanger and pipe geometries, detailed fundamental knowledge of the heat transfer and rheological behaviour needs to be understood. Alongside this, limitations encountered such as stability and supercooling need to be addressed. Within this work, a detailed review of the types of dispersion found in literature, their thermophysical, heat transfer and rheological properties are discussed. Current and past methods of improving formulations and overcoming the aforementioned problems are presented. Furthermore, potential figures of merit to evaluate the efficiency of phase change dispersion utilisation are presented and discussed. An outlook to the existing research gap is given.

## Nomenclature

### Subscripts

$\lambda$	Thermal conductivity ( $\text{W m}^{-1} \text{K}^{-1}$ )
$\mu$	Dynamic viscosity (Pa·s)
$avg$	Average
$b$	Bulk
$C$	Heat capacity rate ratio
$f$	Reference
$gain$	Rate of increase due to PCM addition
$inner$	Inner
$in$	Inlet
$melting$	Melting
$PCD$	Phase change dispersion
$PCM$	Phase change material
$p$	Paraffin
$total$	Total

\*Corresponding author

 [jocelyn.bonjour@insa-lyon.fr](mailto:jocelyn.bonjour@insa-lyon.fr) (J. Bonjour)

ORCID(s):

51 *turbulent* Turbulent

52 *water* Water

53 *w* Wall

54 **Latin Characters**

55 *A* Area ( $\text{m}^2$ )

56 *a* Thermal diffusivity ( $\text{m}^2 \text{s}^{-1}$ )

57 *C* Capacity ratio (-)

58 *c<sub>p</sub>* Specific heat capacity ( $\text{J kg}^{-1} \text{K}^{-1}$ )

59 *c<sub>p</sub><sup>\*</sup>* Modified Specific heat capacity ( $\text{J kg}^{-1} \text{K}^{-1}$ )

60 *d* Diameter (m)

61 *f* Friction factor (-)

62 *i'* Irreversibility rate (W)

63 *J* Colburn factor (-)

64 *K* Consistency index (-)

65 *L* Latent heat of melting ( $\text{J kg}^{-1}$ )

66 *L \** Latent heat capacity ( $\text{J kg}^{-1}$ )

67 *l* Length (m)

68 *M* Merit number (-)

69 *m* Mass flow rate ( $\text{kg s}^{-1}$ )

70 *n* Fluid behaviour index (-)

71 *Nu* Nusselt number (-)

72 *P* Pumping power (W)

73 *Pr* Prandtl number (-)

74 *Q* Heat transfer rate (W)

75 *q* Heat flux ( $\text{W m}^{-2}$ )

76 *Re* Reynolds number (-)

77 *S* Time derivative ( $\text{K}^2 \text{s}^{-1}$ )

78 *Ste* Stefan number (-)

79 *T* Temperature (K)

80 *x* Distance from inlet (m)

81 *z* Empirical shape factor (-)

82 **Abbreviations**

83	COP	Coefficient of performance
84	FOM	Figure of merit
85	HLB	Hydrophilic-lipophilic balance
86	HTF	Heat transfer fluid
87	LHS	Latent heat store
88	MWCNT	Multi-walled carbon nanotube
89	PCD	Phase change dispersion
90	PCE	Phase change emulsion
91	PCM	Phase change material
92	PEG	Polyethylene glycol
93	PVA	Polyvinyl alcohol
94	US	Ultrasound

#### 95 **Greek Characters**

96	$\beta$	Sphericity factor (-)
97	$\dot{\gamma}$	Shear rate ( $1 \text{ s}^{-1}$ )
98	$\Delta p$	Pressure drop (Pa)
99	$\epsilon$	Heat transfer effectiveness (-)
100	$\lambda$	Thermal conductivity ( $\text{W m}^{-1} \text{ K}^{-1}$ )
101	$\mu$	Dynamic viscosity (Pa·s)
102	$\rho$	Density ( $\text{kg m}^{-3}$ )
103	$\tau$	Shear stress (Pa)
104	$\tau_q$	Time lag of heat flux (s)
105	$\tau_t$	Time lag of temperature gradient (s)
106	$\phi$	Particle volume fraction (-)
107	$\psi$	Mass fraction (-)

## 108 **1. Introduction**

109 Cold technologies are essential for a variety of domestic, commercial and industrial applications. They are em-  
 110 ployed in the preservation of food and medical equipment, comfort cooling in cars, residences and commercial build-  
 111 ings and in the cooling of electronic and industrial equipment. Despite its plethora of usages, the cold energy market  
 112 is an often over-looked energy-consuming sector. The use of energy for space cooling is the fastest growing area of  
 113 energy usage in buildings and it has more than tripled between 1990 and 2016 [1]. Worldwide, almost one fifth of all  
 114 electricity utilised in buildings is used for cooling [1]. Current aims to reduce this electrical usage include technologies  
 115 implemented to increase the coefficient of performance (COP) of cold systems. In recent years, this has involved the  
 116 incorporation of phase change materials (PCM) into cold systems to act as latent heat stores (LHS) [2, 3, 4]. LHS  
 117 exploits the heat of phase change of materials to store and release significant amounts of energy as a material changes



118 phase. The isothermal nature of phase change allows PCM systems to be fine-tuned to temperature-sensitive appli-  
119 cations such as air-conditioning (5 to 15 °C), refrigeration (0 to 4 °C) and freezing (less than 0 °C). However, there  
120 are instances where it is much more efficient to use PCM in the form of particles within another fluid. For example,  
121 where heat transfer rate is to be maximized, and where it is beneficial to have the PCM in a pumpable form. Using  
122 PCM in conjunction with a HTF, generally water, results in a two-phase fluid with a high specific heat capacity [5].  
123 The high specific heat capacity is due to the fluid not only using the sensible heat, as with a normal HTF, but with the  
124 additional latent heat during the phase change process [5, 6]. It is expected that because of this, the fluid will have  
125 better heat transfer characteristics than for a single-phase HTF, within a limited temperature range around the phase  
126 change temperature of the PCM. This is beneficial in a number of applications as improved heat transfer and storage  
127 characteristics, such as an increase in the specific heat capacity, allows for a smaller volumetric flow of the HTF to be  
128 used. This suggests that less pumping power is required in the system and thus smaller thermal resistances are achieved  
129 and therefore higher heat transfer efficiencies [7]. Essentially, this could lower the operational and investment costs  
130 of the cold-chain network. To date, there are a couple of reported usages of PCD that have been implemented into  
131 the cooling network. Fischer et al. [8] retrofitted an existing cooling circuit using PCM dispersed in water as the heat  
132 transfer fluid (HTF) to isothermally cool a machine spindle. Additionally, Shibutani [9] installed microencapsulated  
133 slurries into a pre-existing chiller unit in Narita Airport in Tokyo and found higher storage densities than using water  
134 as the HTF. Despite this, PCD are still to be considered in the developmental stage and are not yet commercialised.

135 To date, there are four different types of fluid incorporated with PCM: ice slurries, clathrate hydrate slurries,  
136 microencapsulated PCM slurries and phase change dispersions (PCD) [10, 5, 11]. The first three suffer from high  
137 operational costs, associated with shape stabilisation and encapsulation. Additionally, they suffer with problems of  
138 stability and consistency during extended cycling periods [10, 5, 11]. On the other hand, PCD, or formerly named in  
139 literature as phase change emulsions (PCE), are dispersions of two immiscible liquids, stabilised with a surfactant. PCD  
140 have simple preparation techniques, smaller thermal resistances (as a result of having no encapsulation shell) and lower  
141 production costs [10, 5, 11]. PCD can be characterised by the size of the dispersed droplets. Currently, there are three  
142 different droplet sizes of the dispersed phase used for cooling purposes; emulsions (1-10 µm), mini-emulsions (20-200  
143 nm) and micro-emulsions (10-100 nm) [12]. These sizes are given as reference values and as discussed by Mclements  
144 [13], other factors, such as preparation technique and thermodynamic stability should be taken into consideration when  
145 assigning categories to emulsion types. Emulsions with droplet sizes above 1 µm are currently the most studied but it  
146 is nano-emulsions that show the most promising characteristics such as long-term stability and low viscosities [14].

147 So far, the integration of PCD into cooling systems has been limited due to a range of both material and heat  
148 transfer limitations. Material properties of the PCM such as supercooling, a phenomenon by which a solution starts  
149 crystallising below its freezing point and therefore requires a lower temperature to freeze, significantly limits the ap-  
150 plication of PCD into cooling systems. Additives, named nucleating agents, are added to dispersions to prevent this  
151 from occurring, however their ability to function after multiple cycles and during storage is unknown. Additionally,  
152 PCD suffer from instability when cycled due to thinning and disruption of the liquid film between droplets (coales-  
153 cence), an irreversible process. Furthermore, to ensure the correct design of heat exchangers and systems with PCD, a  
154 comprehensive understanding of the heat transfer performance of PCD is required. Whilst for single-phase Newtonian  
155 fluids an in depth understanding of heat transfer is known, this is not the case for PCD. Numerical models have been  
156 presented [15, 7, 16, 6], but they are yet to be experimentally validated. Despite this, recent literature and reviews have  
157 almost predominantly focused on the characterisation and heat transfer properties of microencapsulated phase change  
158 material slurries [17, 18, 19, 20, 21]. Whilst, there are some reviews which discuss some properties of phase change  
159 dispersions [22, 19, 23], this present review will focus exclusively on the thermophysical properties, heat transfer per-  
160 formance and rheology of PCD. Specifically, this review will focus on PCD made for cooling applications such as:  
161 HVAC, which as discussed by Huang et al. [24] requires a PCD with a phase change temperature between 0-20 °C,  
162 cooling of machining tools as discussed by Fischer et al. [8] with a temperature range of 20-30 °C, refrigeration with  
163 a phase change temperature of 0-6 °C and furthermore the cooling of electronic equipment which can require a phase  
164 change temperature of up to 50 °C [25, 26].

## 165 2. Phase change dispersions

**Table 1**

The formulation method, components and properties of the PCD discussed in this review, ordered by their relative melting points. It is to be noted that blank spaces were left where the data could not be retrieved.

Reference	PCM (wt.%)	Surfactant (wt.%)	Nucleating agent (wt.%)	Preparation technique	Melting point (°C)	Particle Size
[27]	Tetradecane (30)			Phase incursion method	4.7	51 um
[28]	Tetradecane (20)			Phase inversion temperature method	4.8	180-230 nm
[29]	RT6, RT10, RT20 (30)	Span 60/Tween 60 (6)				
[14]	Tetradecane	Alcohol ethoxylates (1.5)	Paraffin wax (2.5)		5.5, 9.5, 19.9	1-10 um
[30]	RT6 (40)	POE(20), POE(10), POE(20)		D-phase method	5.9	
[31]	RT10 (25)	Tween 20, Tween 40 and Tween 80, Tween 60 (2.5)	RT25		6.1	10-100 um
[24]	R10 (15-75)	Brij 52/Tween 20 (1.25, 2, 2.5, 5)		Mixing film synthesis	8.5	1-10 um
[32]	RT10 (30)	Non-ionic surfactant (2.5)	Nucleating agent (2.5)	Rotor-stator emulsification	9.2	1-10 um
[33]	RT10 (15-75)	1.5	1.5		9.7	1-10 um
[34]	OP10E (30)	Non-ionic surfactant (2.5)	Paraffin wax (2.5)	Rotor-stator emulsification	9.8	1-10 um
[5]	n-hexadecane (10,20,30,40)	Tween 80/Span 80 (3,4,5,6,7)	Graphite nanoparticles (0.25, 0.5, 1, 2, 4)	Rotor-stator emulsification	10	1-15 um
[35]	n-hexadecane (10, 20)	Span 80/Tween 80		D-phase method	15.9	70-750 nm
[15]	n-hexadecane (10,20,30)	Span 80/Tween 80		D-phase method	16.2	100-1000 nm
[36]	n-hexadecane	Tween 20/1,3-butandiol (2,4,8)		Rotor-stator emulsification	16.5	200-600 nm
[37]	n-hexadecane (10)	SDS/Tween 40		Ultrasound disperser/Rotor-stator emulsification	16.5-17.5	1-50 um
[38]	n-hexadecane (15)	Tween 60, Tween 80, 1-3-butandiol		Rotor-stator emulsification	17	2.2 um
[39]	n-hexadecane	Brij L4 (5-15)	Hydrophobic SiO <sub>2</sub> nanoparticles (13)	Low-energy phase inversion emulsification	18	100-1000 nm
[14]	n-hexadecane	SDS (2)		Microfluidic droplet production	18	19-40 um
[40]	n-hexadecane	POE(20), POE(10), POE(20)		D-phase method	18.2	
[41]	n-hexadecane (30)	Tween 20(5)/Tween80(5)//SDS(1)	Multi-walled carbon nanotubes (0.05-0.8)	Ultrasound probe/Rotor-stator emulsification	18.5	0.1-20 um
[42]	n-heptadecane, RT21HC (2,4,10)	Tween 20, Tween 80, Span 20, Span 80 (5)	Hydrophobic SiO <sub>2</sub> nanoparticles (2)	Phase inversion temperature method	20.2	800-1200 nm
[8]	RT25HC	SDS (0.25, 0.5, 1.25)	n-octacosane, RT55, RT70HC	Solvent-assisted method	20.5	100-150 nm
[5]	n-octadecane (10,20,30,40)	C16/18 ethoxylated alcohols	Myristic acid (0.5-5)	Rotor-stator emulsification	25	1 um
[15]	n-octadecane (10,20,30)	Span 80/Tween 80		D-phase method	25.5	100-1000 nm
[10]	n-octadecane (10, 20)	Tween 20/1,3-butandiol (2,4,8)		Rotor-stator emulsification	25.5	150-500 nm
[7]	OP28E (10, 20)	SDS (10)	Multi-walled carbon nanotubes, octadecanol (0.1-1.0)	Ultrasonic emulsification	26	58-255 nm
[14]	n-octadecane	SDBS (2, 4)			26.2	180-191 nm
[43]	n-octadecane (30)	POE(20), POE(10), POE(20)		D-phase method	27	
[6]	n-eicosane (1-10)	Triton X100, Tween 60, Span 60 (3)	Polyvinyl alcohol	Rotor-stator emulsification	27.5	2-10 um
[44]	n-eicosane (1,2,5, 10)	SLS			34.7	
[16]	Crodatherm47/Crodatherm 53 (16)	Steareth-100/Steareth-2 (4)	Nucleating agent (0.5)	Ultrasonic emulsification	36.3	50-140 nm
[45]	Stearic acid/Myristic acid (1, 3, 5)	SDS, Span85		Rotor-stator emulsification	49.5	0.1-10 um
[46]	Paraffin wax (10, 20, 50)	Pluronic P-123		Phase inversion temperature method	53	10-100 nm
[11]	Paraffin (20)	PVA/PEG-600 (4)		Probe ultrasonication	57.9	200-600 nm
[47]	n-hexadecane	Brij 35, Brij 52, Brij 58, SDS, Tween (20,40,60)		Rotor-stator emulsification	59	0.1-60 um
[48]	n-hexadecane, n-octadecane	Tween 80		Rotor-stator emulsification		
[49]	n-decane (1, 2, 3, 5)	Span 85/Tween 20 (0.5, 1.5, 2, 3)		High-speed stirring		
				Ultrasonic emulsification		18-110 nm

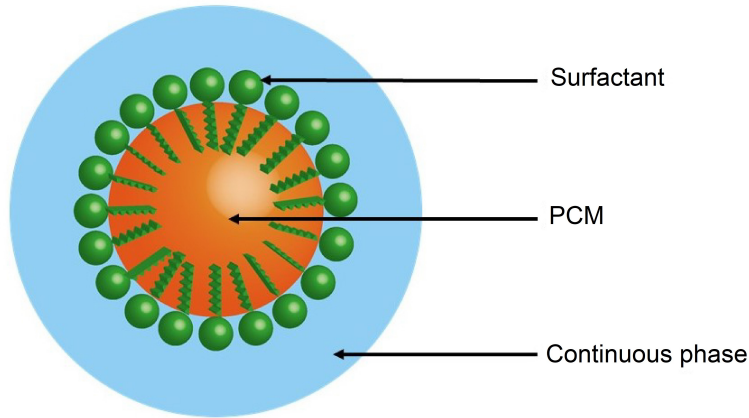


**Figure 1:** A dispersed particle within a PCD showing the PCM, surfactant layer and the continuous phase. The figure was adapted from Fischer et al. [8].

166 As aforementioned, a PCD consists of a dispersed phase which is composed of PCM particles that are stabilised  
 167 and dispersed in a continuous phase with the aid of surfactants. A diagram of a typical PCD droplet can be seen in  
 168 Figure 1 and a list of the formulation properties and components of the PCD discussed in this review can be found  
 169 in Table 1. The most commonly investigated PCDs are oil-in-water, where a hydrophobic PCM is dispersed in a  
 170 hydrophilic (generally water) continuous phase. In literature, the most commonly reported class of PCM for use in  
 171 PCD are paraffins, on account of their high latent heats. In Table 2, a list of some of the PCD investigated in literature  
 172 can be found. Table 2 is ordered based on increasing melting point of the PCD, it also shows (when presented by the  
 173 author of the study) the thermal conductivity, in both the emulsion form (when the PCM is liquid) and suspension  
 174 form (when the PCM is solid), the mean particle size of the PCM droplets in the PCD, the viscosity in emulsion and  
 175 suspension form, and the latent heat capacity of the PCD. The latent heat capacity of a PCD is defined as:

$$L^* = \psi L \quad (1)$$

176 where  $\psi$  is the mass fraction of PCM used in the PCD and  $L$  is the latent heat of melting. Table 2 also highlights a  
 177 range of commercial PCM, which have also been investigated for use as PCD. Due to the distinctive melting points  
 178 of paraffins, and because of the high cost for pure paraffins, many commercial PCM paraffins are blends of different  
 179 paraffins to obtain the desired application temperatures.

**Table 2**  
PCD listed in literature alongside the PCM used in the formulation, ordered on increasing melting temperatures with some relevant thermophysical properties.

PCM	Melting Temperature (°C)	wt. %	$\lambda$ suspension (W m <sup>-1</sup> K <sup>-1</sup> )	$\lambda$ emulsion (W m <sup>-1</sup> K <sup>-1</sup> )	Mean Particle size ( $\mu$ m)	$\mu$ suspension (mPa s)	$\mu$ emulsion (mPa s)	Latent heat capacity (J g <sup>-1</sup> )	[Ref]
Tetradecane	4.6	30			51		7.5	73	[27]
Tetradecane	4.8	20			0.2		4.2	43	[28]
n-alkanes	5	30	0.38			7.3	5.5	60	[50]
Tetradecane	5.9	10			0.5			19.3	[14]
Tetradecane	6	40			17			66.3	[51]
RT6	6.1	30		0.48		10	25	40	[30]
RT6	8	30			0.5	20	20	75	[29]
RT10	8.2	25	0.4		4		21	41	[31]
RT10	9	30			5			43	[32]
RT10	9.3	30			5			36	[24]
n-alkanes	9.5	50			2	24.3	22.3	78.9	[52]
RT10	9.7	30		0.46				38	[30]
RT10	10	30			0.5	40	20	50	[29]
Hexadecane	16.5	10			100				[53]
Hexadecane	17.5	10	0.56	0.54	0.2	2.9	1.7	22.9	[15]
Hexadecane	17.5	20	0.52	0.48	0.3		4.1	45.8	[15]
Hexadecane	17.5	30	0.49	0.47	0.3		16.5	68.7	[15]
Hexadecane	18.2	10			0.5				[14]
Hexadecane	19.4	50			1.8		45	73.4	[40]
RT20	22	30			0.5	80	20	44	[32]
RT25HC	23	26			1			41	[8]
Octadecane/Hexadecane (50:50)	24	16	0.52	0.48	0.3	4.4	3.1	24	[54]
Octadecane	27	10	0.5	0.45	0.5				[14]
Octadecane	27.2	10	0.56	0.54	0.18	3.4	1.8	24.3	[15]
Octadecane	27.2	20	0.52	0.48	0.2		4.1	48.6	[15]
Octadecane	27.2	30	0.49	0.41	0.23			72.9	[15]

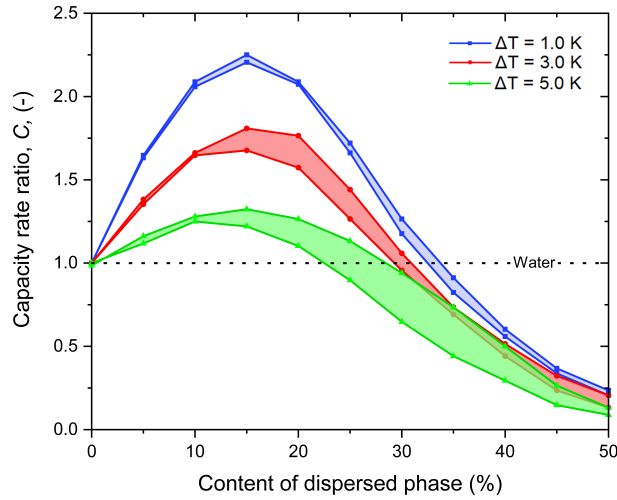


**Figure 2:** Heat capacity rate ratio,  $C$ , for a laminar flow in a pipe versus mass content of PCM within the PCD,  $\psi$ , based on Equation 2. For each assumed temperature difference,  $\Delta T$ , (1, 3 and 5 K), the two curves of the same colour show the upper and lower limits of  $C$ . The two limits are calculated from:  $T_{melting} \pm \Delta T$ , where  $\Delta T = 1, 3, 5$ . The figure was adapted from Fischer et al. [56]

180 Paraffins however, are derived from non-sustainable oil feed stocks and can be flammable [55]. In recent years,  
 181 research has focused on finding more sustainable PCM for PCD. Zhang et al. [40] investigated fatty acids, on accounts  
 182 of their abundance, low cost, chemical inertness and non-toxicity. Four mixtures of fatty acids and eutectics thereof,  
 183 were investigated. The thermophysical properties of the fatty acids as PCM can be found in [40]. From literature  
 184 studies, 30 wt.% of the dispersed phase is most commonly investigated (see Table 2). Huang et al. [24] studied different  
 185 weight percentages of paraffin dispersions and found 30 wt.% to be the minimum paraffin content for a specific heat  
 186 capacity to be twice that of water during melting. However, Fischer et al. [56] found that 15 wt.% was optimal when  
 187 considering the capacity rate against the content of dispersed phase, where the capacity rate ratio for a laminar  
 188 flow regime is defined to be:

$$C = \frac{\mu_{water} c_{p,PCD}}{\mu_{PCD} c_{p,water}} \quad (2)$$

189 where  $\mu_{water}$  and  $\mu_{PCD}$  are the dynamic viscosities of water and the PCD respectively and  $c_{p,PCD}$  and  $c_{p,water}$  are the  
 190 specific heat capacities of the PCD and water respectively. Figure 2 shows the capacity rate ratio,  $C$ , against the mass  
 191 content of the PCM in the PCD, where it can be observed that a maximum  $C$  is obtained at 15 wt.%.

### 192 3. Physical properties

193 There are certain criteria that a PCD must fulfil to be considered useful as a HTF. These criteria include [56, 14,  
 194 57, 58]:

- 195 • high specific heat capacity (generally listed as twice that of water for the desired temperature range)
- 196 • high latent heat capacity
- 197 • high heat transfer rate
- 198 • low pressure drop in operation
- 199 • high storage stability
- 200 • high stability under thermal and mechanical loads during cycling

- high phase change enthalpy
- small degree of supercooling

These criteria will be discussed in the following sections of this review.

### 3.1. Stability

PCD should demonstrate long-term stability, both in storage and under shear stress thermal cycling. A dispersion is considered stable if there is no distinct growth in droplet size over continuous cycling or if there is no phase separation during storage of the dispersion [34, 10, 38]. There are currently five known mechanisms by which dispersions can destabilise: creaming, sedimentation, coalescence, Ostwald ripening and phase inversion [58]. These mechanisms of destabilisation are outlined in Figure 3. Oftentimes, destabilisation mechanisms are accelerated by thermal and mechanical cycling, which is why it is extremely important for researchers to focus on investigating stability over multiple thermal cycles. Within oil-in-water dispersions, the most commonly observed mode of destabilisation is creaming, due to oils (typically paraffins) having lower densities than water [15, 5]. Abedi et al. [39] stated that there are two major shortcomings in studying the stability of dispersions and that is the indirect measurement techniques and polydisperse droplet sizes. To overcome this, Abedi et al. [39] produced dispersions with controlled and narrow particle size distributions using microfluidics. Zou et al. [59] suggested two methods for overcoming the destabilisation of dispersions, the first is to use an optimal concentration of PCM in the dispersion. High concentrations of PCM have a greater probability for agglomeration or precipitation, but reducing the concentration of PCM significantly will reduce the total heat capacity of the dispersion [59]. The second method proposed by Zou et al. [59] is in accordance with Stokes law. Stokes law predicts that a stable dispersion will have a high viscosity, small density difference between the two phases and small droplet diameters. From these properties, reducing the droplet size is the most feasible. Zou et al. [59] stated that reducing the droplet size causes a large reduction in the gravitational force in the dispersion, suggesting that the Brownian motion may overcome the gravitational force. It has been suggested that PCD with droplet sizes between 20-500 nm offer high stabilities and have greater longevity [41, 36]. Huang et al. [24] additionally discovered that creaming can be reduced by decreasing the droplet size of dispersions or increasing the viscosity of the dispersion. This was also found by Zhang et al. [41]. The greater stability of more viscous continuous phases was attributed to the retardation of aggregation of the PCM droplets. Lu and Tassou [30] used Xanthan gum as a thickener and found a reduced creaming destabilisation in their PCD. Despite this, for practical use thickeners cannot be used in industrial or commercial PCD systems due to the increased pumping power needed to pump a more viscous fluid. Abedi et al. [39] found that dispersions with a smaller droplet size are more stable due to the probability of particle coalescence being reduced. Despite this, smaller droplet sizes are associated with higher PCD viscosities for a given mass or volume of fluid and also an increased supercooling [24]. It is suggested by the author of this review that a compromise on droplet size should be reached to ensure good stability, low viscosities and lower supercooling degrees. Surfactants are often used to prevent instability in emulsions. From a literature search, it can be found that quite a large range of surfactants have been utilised to prevent destabilisation. Tween variations, which are non-ionic poly-ethoxylated surfactants, are commonly used for oil-in-water dispersions. Golemanov et al. [47] used a series of Tween surfactants (Tween20, 40, 60 and 80) and compared them to other surfactants. It was concluded that Tween 40 and Tween 60 were the most effective surfactants at stabilising paraffin-in-water dispersions, which was attributed to the fact that their chain length was small enough to allow the formation of dense interfacial layers surrounding the PCM, which were stabilised due to the steric effect [47]. Lu and Tassou [30] showed that non-ionic surfactants were better than ionic surfactants for dispersion stability and additionally reducing toxicity. More recently, this was confirmed by Chen and Zhang [5]. Tokiwa et al. [60] found that the concentration of the surfactant is also an important factor when considering PCD stability as the concentration of surfactant needs to be sufficient to ensure the entire surface of the PCM droplets are coated.

To select the appropriate surfactant for a specific system, the Hydrophilic-Lipophilic balance (HLB) should be calculated [26]. For oil-in-water emulsions, a HLB of between 8 and 18 has been suggested. For a paraffin-in-water dispersion though, a narrower range of 11.8-12.0 was suggested by Orafidiya and Oladimeji [61]. This was also suggested by Xu et al. [62] who investigated both the optimal paraffin concentration and surfactant type and concentration for maximum stability of a tetradecane-in-water dispersion. Therefore, to meet the stringent HLB of 12.0, often two or more surfactants are combined. For example, Chen and Zhang [5] investigated a dispersion using a combination of Span 80 and Tween 80 in hexadecane and octadecane-in-water dispersions with 1,3-butanediol to reach a HLB of 12.0. Shao et al. [31] used Brij 52 and Tween 60, with an overall HLB of 12.0, for a paraffin based PCD and the PCD showed

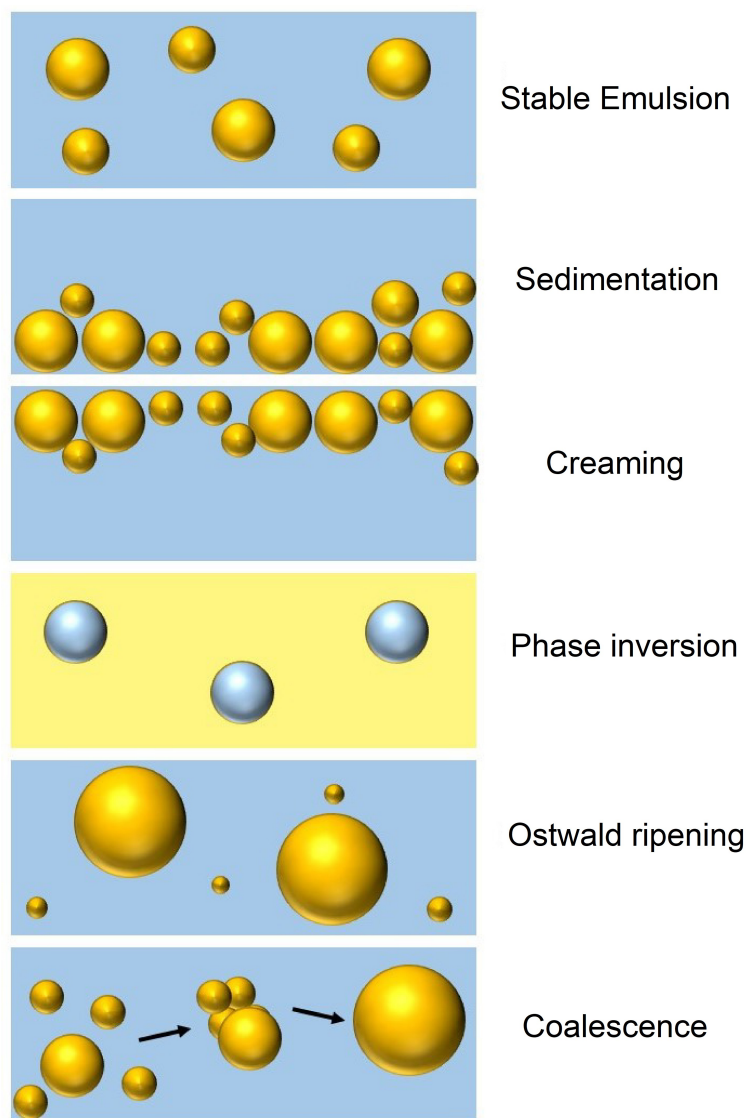


**Figure 3:** Schematic showing a stable emulsion alongside the destabilisation mechanisms.

252 good stability. Zhang et al. [41] further suggested that polymeric surfactants added as co-surfactants to the emulsifier  
 253 system could increase PCD stability. Co-surfactants can be used to increase the interfacial strength between surfac-  
 254 tants and PCM droplets. This method was also tested by Wang et al. [11] who tested a polymer surfactant mixture of  
 255 PVA and PEG and found that stable emulsions were created. This was also discovered by Kawanami et al. [14] who  
 256 added 1,3 butanediol and ethylene glycol as co-surfactants to increase the stability. Furthermore, the surface charge  
 257 (Zeta potential) is also an important parameter to consider for a PCD's stability [63]. Measuring the Zeta potential of  
 258 PCD measures the electrophoretic mobility of the PCM droplets and if the absolute value of the Zeta potential is over  
 259 30 mV, there is a strong indication that the electrostatically repulsive charges between the PCM droplets are strong  
 260 enough to prevent agglomeration and coalescence [42]. This parameter is controlled by the concentration and type of  
 261 surfactant used. Pupponen et al. [45] investigated the Zeta potentials of different concentrations of two surfactants,  
 262 individually and as co-surfactants in fatty acid based PCDs. Pupponen et al. [45] found that a 1:1 ratio of SDS and  
 263 Span85 resulted in the highest zeta potential of -78 mV. They also discovered that increasing the ratio of surfactant to  
 264 dispersed phase increased the Zeta potential and thus the stability against coalescence. Cabaleiro et al. [42] measured  
 265 the Zeta potentials of RT21HC in water PCD stabilised with SDS surfactants to be -71 mV. Cabaleiro et al. [64] also



performed another investigation with RT21HC in water, with varying concentrations of SDS surfactant; 0.25, 0.5 and 1.25 wt.% and it was found that in all cases a Zeta potential of -80 mV was achieved, suggesting that the electrostatic charges were strong enough to prevent coalescence. Jadhav et al. [65] slowly increased the concentration of the SDS surfactant used in their paraffin wax PCD from 0-10 mg ml<sup>-1</sup> and found a corresponding zeta potential drop from -38.1 mV to 38.8 mV. This was attributed to a higher surface charge caused by an increase in the number of surfactant molecules around each paraffin droplet which improved the stability.

### 3.1.1. Stability during storage

Huang et al. [24] stated that the most important factor to take in consideration when trying to increase PCD stability is PCM concentration. They found that after one month, distinct layering was observed in PCDs containing 16-60 wt.% paraffin, but creaming was not evident in the dispersions with 65-75 wt.% paraffin. However, practically, PCD with such high paraffin concentrations cannot be used in cooling systems as a result of the high viscosity associated with PCD with higher PCM concentrations. Günther et al. [36] prepared a 30 wt.% hexadecane dispersion and found that creaming occurred in only a few days. Another study performed by Huang et al. [29] found that after two years of storage, no significant destabilization was observed. Chen and Zhang [5] investigated the effect of HLB on the storage stability of their PCD and found that a dispersion with a HLB of 12.0 had a stabilisation period of greater than 210 days, but a dispersion with a HLB of 15.0 began to destabilise after 65 days. Despite this, Shao et al. shao2016 still found that after a storage period of 270 days there was an increased mean droplet size from 3.1  $\mu\text{m}$  to 3.4  $\mu\text{m}$  which was indicative that coalescence had occurred. Fischer et al. [26] showed that when their PCD was below its melting temperature (suspension form), the lifespan was 300 days, and when it was above its melting temperature (emulsion form), the lifespan was 25 days. Cabaleiro et al. [42] produced PCD with droplet sizes between 90 - 120 nm and it was found that after 30 days in storage, the average droplet diameter had not increased, suggesting high stability. This was attributed to the droplets being small enough that Brownian motion ensured that the droplets moved throughout the sample and didn't cream to the top of the sample during storage [42]. As discussed by Chen and Zhang [5], who formulated nanoscale PCD, smaller particle sizes tend to improve the stability of dispersions, however they also increase viscosity and degree of supercooling.

### 3.1.2. Stability during cycling

Huang et al. [24] performed cycling tests on a PCD with 35 wt.% paraffin, 2.5 wt.% surfactant and 2.5 wt.% nucleating agent. The cycling involved a heating/cooling cycle, which was repeated 50 times for 6 days. They found that the particle sizes slightly increased after cycling, and supercooling was observed. It was assumed by the authors that this was due to the nucleation agent separating from the dispersion. It was concluded however, that due to the viscosity remaining the same throughout cycling, that the PCD was stable to mechanical and thermal cycling. This was attributed to the mechanical energy provided in the pumping system preventing creaming from occurring. Another study by Huang et al. [29] found that dispersions of 30 wt.% RT10 and RT20 respectively also had an increased particle size distribution after thermal-mechanical cycling. Schalbart et al. [28] investigated the preparation methods of dispersions and their effects on stability. It was found that methods, which produced a narrow droplet size distribution, generated dispersions that were stable against creaming for more than 6 months, however during cycling Ostwald ripening was observed which increased the droplet size and decreased the viscosity. Additionally, it has been suggested by Wang et al. [11] that the addition of co-surfactants ensures good stability of the dispersion. They found that a mass ratio of 50:50 PVA to PEG-600 had good stability after 50 cooling-heating cycles. Although not applied specifically to PCD systems yet, research in emulsion chemistry has found that Pickering emulsions could offer increased stabilisation in PCD. This involves stabilising the surfactants with amphiphilic solid nanoparticles [41, 38]. More recently however, alternative additives, other than surfactants are being used to safeguard the stability of emulsions and prevent against creaming, for example, Zhang et al. [41] concluded that the addition of SiO<sub>2</sub> nanoparticles increased the stability of a paraffin-in-water emulsion.

## 3.2. Supercooling

For a material to crystallise, nucleation must occur. However, the process of nucleation has a potential energy barrier, which must be overcome for nucleation and thus crystallisation to initiate. This energy barrier is a function of the radius of a nucleus formed in the solution and it is not until a critical radius is reached that the energy barrier can be overcome and nucleation is initiated [66]. However, if a nucleus is smaller than this critical radius, nucleation will not occur, as the nucleus will collapse. The process of nucleation and supercooling is discussed extensively in



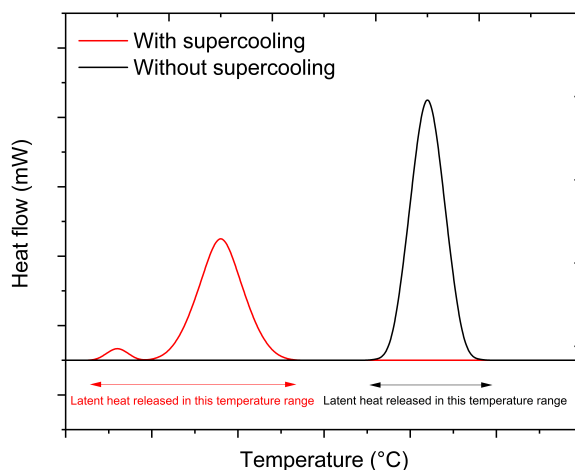


**Figure 4:** Example of a DSC curve showing the crystallisation curves of two PCD, the solid black line shows an "ideal" PCD with no supercooling, whereby the latent heat is released over a small  $\Delta T$ . The red dashed-line shows a PCD with supercooling, whereby the latent heat is released over a broad temperature range.

[67]. The barrier to nucleation though, can also be overcome through thermal energy fluctuations, which are stochastic events that render nucleation a probabilistic phenomenon [68]. Because of this, nucleation is highly dependent on temperature. There are two kinds of nucleation, homogeneous and heterogeneous. Homogeneous nucleation occurs in an ideally pure solution, where no external contaminants can act as heterogeneous nucleators. Due to the stochastic nature of homogeneous nucleation, a larger volume of material suggests a higher probability for nucleation to occur. However, within a dispersion, the PCM volume is dramatically reduced compared to a bulk solution, hence reducing the likelihood of homogeneous nucleation occurring, resulting in large supercooling degrees. This is particularly obvious in the case of nano-sized emulsions, whereby in the small and isolated droplets, the probability of their being an external contaminant is lower, and thus crystallisation proceeds via homogeneous nucleation [42].

It is well observed that large degrees of supercooling limit the applications of PCD in cooling systems as the latent heat contributing to the large heat capacities of dispersions is released over a broad temperature range, rather than being released as a sharp peak over a narrow temperature range, this is outlined in Figure 4. Figure 4 shows an example of a typical DSC curve for crystallisation of two different PCD, one of the curves represents an "ideal" PCD with little to no supercooling, and the other curve represents a PCD with a large supercooling degree. Within PCD, there tends to be large degrees of supercooling, over a broad temperature range, as a result of the different crystallisation temperatures of different PCM droplets within the PCD (as a result of different particle size distributions and local droplet temperatures). A narrow crystallisation temperature of PCM within the PCD is essential for PCD acting as HTF for temperature stability and for applications which require isothermal conditions. Large degrees of supercooling also suggest that the PCM within the PCD crystallises at lower temperatures, meaning a lower temperature from the chiller is required to crystallise the PCM which increases the energy consumption of PCD systems and reduces their efficiency [10]. Methods to combat supercooling have been the centre of PCM and PCD research for quite some time. Huang et al. [24, 29] performed a two part investigation on supercooling in tetradecane and hexadecane dispersions.

### 3.2.1. Effect of droplet size

Huang et al. [24] discovered that a 30 wt.% tetradecane-in-water emulsion with a droplet diameter of 1-10  $\mu\text{m}$  had a supercooling degree of 7 K. Large supercooling degrees were also found by Günther et al. [36], Lu and Tassou [30], Hagelstein and Gschwander [43] and Wang et al. [11]. To investigate the claim that particle size influences the degree of supercooling, Günther et al. [36] prepared dispersions with droplet sizes ranging from 0.2 to 20  $\mu\text{m}$  using different methods, ultrasound and different frequencies. For the smaller droplet sizes, supercooling on the scale of 15 K was observed, and for the larger particle sizes a supercooling of 5 K was observed. Figure 5 shows the nucleation

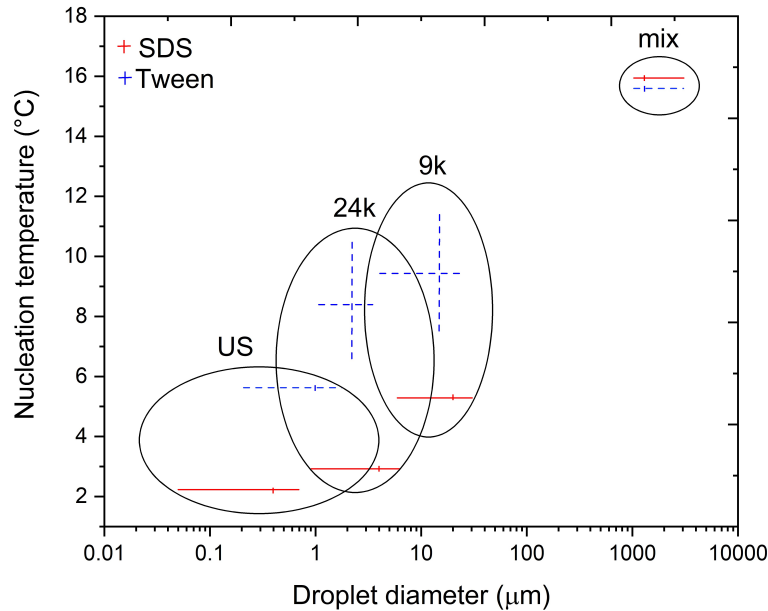


**Figure 5:** Nucleation temperature for hexadecane PCD with varying hexadecane droplet diameters, which were prepared with different methods, ultrasound (US), homogeniser at 24,000 rpm and 9,000 rpm from [36]

345 temperature against droplet diameter for PCD with different production methods and surfactants used. From Figure 5,  
 346 it is evident that the larger the droplet size, the higher the nucleation temperature and thus the lower the supercooling  
 347 degree

### 348 3.2.2. Effect of surfactant used

349 Günther et al. [36] concluded that interfacial phenomena between the surfactant and the PCM has an effect on  
 350 the initiation of crystallisation due to surfactants having a large impact on the thermal properties of the dispersion.  
 351 Functionalising the surfactant ensures that each dispersed particle contains a nucleation seed, therefore suggesting  
 352 that each individual dispersed particle should crystallise. Hagelstein and Gschwander [43] used PVA as a surfactant  
 353 to reduce the supercooling of hexadecane dispersions from 12 K to 2 K. Lu and Tassou [30] also found that using  
 354 hexadecanol, as a co-surfactant, reduced supercooling by 3 K compared to when just Tween 20 was used. Hexadecanol  
 355 was also used by Zhang et al. [40] as a co-surfactant in a capric acid/lauric acid in water dispersion, and here it was  
 356 found that the supercooling degree was reduced from 20 K to 10 K.

### 357 3.2.3. Effect of additives

358 Additives are often added to PCD to induce heterogeneous nucleation. Huang et al. [29] added a paraffin with  
 359 a phase change temperature of 50 (which is a paraffin with a higher melting point than the PCMs used in the PCD)  
 360 to the dispersion as a nucleating agent. Adding a higher melting point paraffin was also found to be effective by  
 361 Lu and Tassou [30]. Zhang et al. [40] used multi-wall carbon nano-tube (MWCNT) particles that resulted in the  
 362 supercooling being reduced by 46% from 6.4 to 3.5 K. Fischer et al. [56] investigated varying amounts of Myristic  
 363 acid in a RT25HC-in-water dispersion and found that increasing the amount of Myristic acid in the PCD decreased  
 364 the degree of supercooling. Furthermore, a time-cycling dependency has been observed on the efficacy of nucleating  
 365 agents, whereby after a certain amount of thermo-mechanical cycles the nucleating agents stops or reduces its impact  
 366 on the crystallisation temperature [26]. It is therefore suggested that these cycling effects of nucleating agents and  
 367 efficacy in reducing supercooling is researched more in depth.

## 368 3.3. Heat Capacity

369 Utilising PCD as a HTF requires an increase in the total heat capacity compared to the specific heat of water  
 370 at the desired application temperature. When comparing the total heat capacity of a PCD with water, the applied  
 371 temperature range (around the phase change temperature) needs also to be considered on an application by application

372 basis, depending on the operational conditions. When considering PCD, the total heat capacity of the PCD is defined  
 373 as [56]:

$$c_{p,PCD,total} = (1 - \psi)c_{p,water} + \psi \frac{L_{melting,PCD}}{\Delta T} \quad (3)$$

374 and is it generally calculated over a 6 K temperature difference around the melting point of the PCM within the PCD  
 375 as found with DSC analysis (unless otherwise stated) [69]. Generally, the  $c_{p,total}$  is higher for PCD than for water as  
 376 a result of the increase in the specific heat capacity during the phase change of the PCM. In fact, it is the increased  
 377 total heat capacities of PCD over single-phase HTF which stands as the basis for the development of PCD. Chen and  
 378 Zhang [5] concluded in their study that due to the high total heat capacity of their PCD, the dispersion was particularly  
 379 attractive for practical applications such as cooling and air-conditioning. This is because, as found in a study by Lu  
 380 and Tassou [30], that amongst other parameters, the total heat capacity was found to have a great influence on the heat  
 381 transfer of the PCD. To increase the total heat capacity, increasing the mass content of PCM within the dispersion is  
 382 effective. Sivapalan et al. [46] found that a 10 wt.%, 20 wt.% and 33 wt.% paraffin wax PCD possessed a total heat  
 383 capacity which was 7, 31 and 43% higher than water respectively. Huang et al. [32] investigated a PCD composition  
 384 of 50 wt.% and 30 wt.% of RT10 which had total heat capacities which were 2.7 and 2.0 times higher than water  
 385 respectively for the applied range of 5-11 °C, i.e a 6 K temperature range. In another investigation, Huang et al. [29]  
 386 found that their Cryosol 6, Cryosol 10 and Cryosol 20 PCDs had a latent heat capacity that was 3 times, 2 times and  
 387 1.8 times higher than that of water respectively, also in a 6 K temperature range. Despite this, increasing the mass  
 388 fraction of PCM decreases the thermal conductivity of the PCD and increases the viscosity, and thus when creating a  
 389 PCD all parameters discussed in this review must be balanced and analysed using figures of merit, which is discussed  
 390 further in section 5.

### 391 3.4. Thermal conductivity

392 Currently, one of the major drawbacks of dispersions is that paraffins have low thermal conductivities therefore  
 393 dispersions in general have lower thermal conductivities than traditional single phase HTF. Shao et al. [31] measured  
 394 the thermal conductivity of a 25 wt.% RT10 in water PCD to be 30% less than water at the same temperature. Whilst  
 395 an increase in thermal conductivity is not necessary in terms of heat transfer into the dispersed particles to melt them  
 396 (due to their small size), it is important in terms of the overall heat transfer mechanism within PCD. Currently, this is  
 397 unknown and therefore represents a major research gap in the study of PCD. It has also been stated that the thermal  
 398 conductivity of PCD varies non-linearly with the size of the PCM droplets, concentration of PCM, fluid properties  
 399 and temperature, making correlations for describing the thermal conductivity difficult to produce [48]. Yu et al. [70]  
 400 explained that the thermal conductivity of dispersions depends not only on the concentration of the PCM within the  
 401 dispersion but is a complex mixture of: the particle size and distribution, the particle shapes and orientations, the  
 402 Brownian motion of the droplets, the aggregation of the droplets, the dispersions continuous phases's interfacial layer,  
 403 additives, pH and temperature. This section will further explore the effects of different parameters on a dispersion's  
 404 thermal conductivity.

#### 405 3.4.1. Effect of PCM concentration

#### 406 3.4.2. Effect of phase change

407 The operational temperature of the PCD has an influence on the thermal conductivity for example, Wang et al.  
 408 [11] found that for a 20 wt.% dispersion, the thermal conductivity at 30 °C was 0.49 W m<sup>-1</sup> K<sup>-1</sup> and at 60 °C was  
 409 0.61 W m<sup>-1</sup> K<sup>-1</sup>. However, phase change has a significant impact, after the PCD melts, there is a sharp decrease in  
 410 the thermal conductivity due to the decreased thermal conductivity of liquids compared to solids. Chen and Zhang [5]  
 411 found a large decrease in the thermal conductivity at the melting temperature, due to the PCM changing phase from  
 412 a solid to a liquid. It has also been suggested that the thermal conductivities of dispersions have been overestimated  
 413 during melting, due to the large amount of heat absorbed by the dispersion under isothermal conditions [62]. Figure 6  
 414 shows the significant decrease in the thermal conductivity during melting of two different dispersions prepared in [5].

#### 415 3.4.3. Effect of droplet size

416 Additionally, experimental work by Liu et al. [71] highlighted that the thermal conductivity of paraffin-in-water  
 417 dispersions vary with the PCM droplet size and that the thermal conductivity can be increased by reducing the droplet  
 418 size. However, it should be noted that droplet size should be chosen when taking into consideration other factors such  
 419 as supercooling, stability and viscosity.

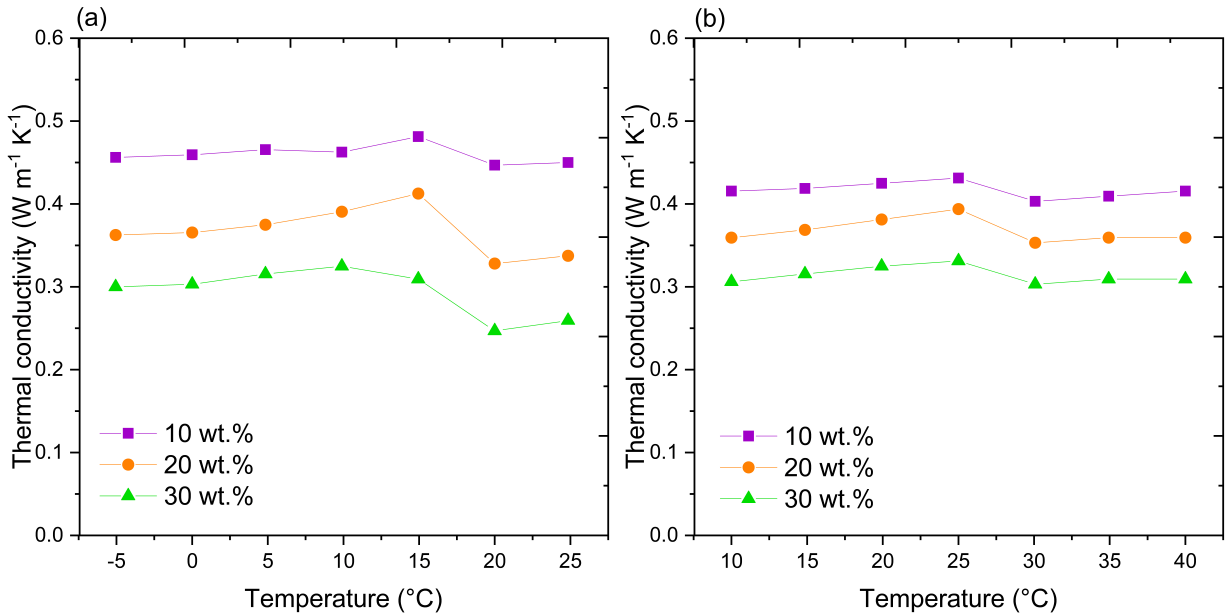


**Figure 6:** Variation of the thermal conductivity of (a) a hexadecane-based PCD and (b) an octadecane-based PCD at different temperatures and weight percentages of the dispersed PCM. Figure was adapted from Chen et al. [5].

#### 3.4.4. Effect of additives

Current methods to increase the thermal conductivity of dispersions involve the addition of nanoparticles. For example, Zou et al. [59] investigated adding 1 wt.% of aluminium nanoparticles into a paraffin emulsion and found a 30% increase in the thermal conductivity, so that the thermal conductivity almost rivalled that of pure water. Ho and Gao [72] added 5 and 10 wt.% of  $\text{Al}_2\text{O}_3$  nanoparticles which showed a 2 and 6% increase in the thermal conductivity of the PCD compared to without the nanoparticles. At 60 °C, an increase in 17% of the thermal conductivity was achieved, which was suggested by the authors to be due to the enhanced Brownian motion with the addition of the nanoparticles in the base fluid having a much lower viscosity at increased temperatures [72]. However, it has been noted that the addition of nanoparticles adds extra cost and reduces the fraction of paraffin used (and thus the total heat capacity) and as a result have been rendered unsuitable for use in most dispersion systems. Ho and Gao [72] found that by adding 10 wt.% of  $\text{Al}_2\text{O}_3$ , that the latent heat of fusion decreased from  $243 \text{ kJ kg}^{-1}$  (with no nanoparticles) to  $212 \text{ kJ kg}^{-1}$ .

#### 3.4.5. Calculating the thermal conductivity of PCD

Due to the different components in PCD having different thermal conductivities, equations have been produced from researchers to quantify the effective thermal conductivities of PCD for different mass fractions of PCM used. The effective thermal conductivity is most often calculated by modified versions of the first-order approximation Maxwell equation [73]:

$$\lambda_{PCD} = \frac{\lambda_{PCM} + 2\lambda_{water} + 2(\lambda_{PCM} - \lambda_{water})\phi}{\lambda_{PCM} + 2\lambda_{water} - 2(\lambda_{PCM} - \lambda_{water})\phi} \lambda_{water} \quad (4)$$

where  $\lambda_{PCD}$ ,  $\lambda_{PCM}$ ,  $\lambda_{water}$  are the thermal conductivities of the dispersion, PCM and water respectively and  $\phi$  is the particle volume fraction. The Maxwell equation is an empirical equation based on the effective medium theory. It has been suggested by Cabaleiro et al. [42] that the Maxwell equation does not take into account scale-related phenomena, for nano-sized PCM droplets which include; interfacial resistance, Brownian motion, droplet-continuous phase interactions or the flow of the droplets.

442 Kawanami et al. [14] used the Hamilton and Crosser equation to evaluate the thermal conductivity [74]:

$$\frac{\lambda_{PCD}}{\lambda_{water}} = \frac{(\lambda_{PCM} + (z-1)\lambda_{water} - (z-1)\phi(\lambda_{water} - \lambda_{PCM}))}{(\lambda_{PCM} + (z-1)\lambda_{water} + \phi(\lambda_{water} - \lambda_{PCM}))} \quad (5)$$

443 where  $z = 3/\beta$  and  $\beta$  is a sphericity factor, which was assumed to be 1. Within literature, it has been noted that an  
 444 increase of thermal conductivity exists in oil-in-water dispersions and that this increase, alongside droplet size has not  
 445 been considered in current equations for calculating the effective thermal conductivities of PCD [71]. However, Liu  
 446 et al. [71] proposed a new semi-empirical equation of the effective thermal conductivity, which takes into account the  
 447 droplet size of the PCM [71]:

$$\lambda_{PCD} = \frac{(\lambda_{PCM} + 0.9023\lambda_{water} + 0.0051\phi(\lambda_{water} - \lambda_{PCM}))(1 + 0.0512\frac{T}{T_f})(1 - 0.0215\frac{d_{PCM}}{d_{water}})}{(\lambda_{PCM} + 0.8699\lambda_{water} + 1.6824\phi(\lambda_{water} - \lambda_{PCM}))(1 + 0.00194\frac{T}{T_f})(1 - 0.0001\frac{d_{PCM}}{d_{water}})} \quad (6)$$

448 for the following conditions:  $20\text{ }^\circ\text{C} \leq T \leq 70\text{ }^\circ\text{C}$ ,  $0.5\% \leq \phi \leq 4.0\%$ ,  $0.5\text{ }\mu\text{m} < d < 0.9\text{ }\mu\text{m}$  where  $T_f$  is the reference  
 449 temperature of  $20\text{ }^\circ\text{C}$ . Liu et al. [71] investigated the dual-phase-lag heat conduction which combines the micro-  
 450 structural effects occurring between PCM droplets into delayed temporal responses into the macroscopic formulation  
 451 of the entire PCD. The dual-phase lag heat conduction was quantified based on the time lag ratio suggested by Kang  
 452 et al. [75]:

$$\frac{\tau_q}{\tau_t} = \frac{S\pi\lambda^2}{4aq^2} \quad (7)$$

453 where  $\tau_q$  describes the thermal inertia in short-time responses,  $\tau_t$  is the delayed time caused by heat transport mech-  
 454 anisms in micro-scale,  $S$  is the time derivative,  $q$  is the heat flux and  $a$  is the thermal diffusivity. When  $\tau_q/\tau_t > 1$  the  
 455 governing equation of the dual-phase-lag heat conduction is hyperbolic and therefore is transported by thermal waves.  
 456 When  $\tau_q/\tau_t < 1$  the thermal conductivity is dominated by non-Fourier heat conduction and when  $\tau_q/\tau_t = 0$ , the gov-  
 457 erning equation is the classical diffusion equation employing Fourier's law. Liu et al. [71] found all their investigated  
 458 dispersions had  $\tau_q/\tau_t$  between 0.1 and 0.3 suggesting that a diffusion-dominated non-Fourier heat conduction could  
 459 exist in oil-in-water emulsions. Further investigation into this for other dispersions is suggested by the authors.

### 460 3.5. Rheology and viscosity

461 It is important to investigate the rheology of dispersion systems as viscosity influences the heat transfer, stability  
 462 and pumping power requirements of dispersions [8]. Delgado et al. [76] showed that due to the high viscosity of their  
 463 60 wt.% paraffin in water dispersion, the natural convective heat transfer was highly reduced. Additionally, Chen et al.  
 464 [27] found that PCD had higher viscosities than water, which led to drastic increases in the required pumping power  
 465 in their feasibility studies. Increased viscosities of PCD has also shown to increase the pressure drop in comparison to  
 466 water [5, 11]. Wang et al. [11] found that although the PCD had double the storage capacity of water, due to the higher  
 467 viscosity and thus higher pressure drop of the PCD, the power consumption for the PCD system was found to be higher  
 468 than for water. This increase in viscosity was originally attributed to solely the weight percentage of PCM employed,  
 469 with an increasing concentration of PCM leading to an increased viscosity. For example, Ho et al. [44] investigated  
 470 1-10 wt.% n-Eicosane-in-water dispersions and reported pressure drops which were up to 200% for 10 wt.% compared  
 471 to 1 wt.% highlighting the dependency of the pressure drop and viscosity on the concentration of the dispersed phase.  
 472 However, more recently it has been suggested that the temperature the PCD is operated at and the concentration of  
 473 surfactant are two other important factors [40, 30]. These results are promising as it suggests that PCD can be  
 474 fine-tuned to create compromised rheological properties whereby optimising the composition of the PCD allows for  
 475 smaller viscosities and pressure drops whilst still retaining high heat transfer properties and stabilities. The majority of  
 476 the dispersions tested in literature show extremely high viscosities compared to water, for example, Inaba and Morita  
 477 [77] produced a 5 wt.% and 40 wt.% tetradecane-in-water emulsion and found the dispersions had viscosities of 31.1  
 478 mPa-s and 2.5 Pa-s, which are 1167 and 21 times higher than the viscosity of water respectively. Additionally, Zhao  
 479 and Shi [78] found dispersions of 16 wt.% and 50 wt.% tetradecane-in-water had apparent viscosities of 24.5 mPa-s  
 480 and 150 mPa-s which is 16 and 100 times the apparent viscosity of water respectively. Shao et al. [31] also observed a  
 481 viscosity for a 30 wt.% paraffin-in-water dispersion, which was 13 times higher than that of water. The high viscosities  
 482 of these dispersions render them unviable for HVAC and cooling applications due to the increase in the pump energy

consumption. Additionally, this causes a switch from the turbulent to laminar flow regime resulting in a decreased heat transfer coefficient. However, more recently, Chen et al. [27] prepared a PCD with 30 wt.% paraffin and found a viscosity of 8.46 mPa·s which is only 5.6 times higher than water.

### 3.5.1. Effect of PCM concentration

One of the most well-known and investigated factors in the viscosity of dispersions is the concentration of the dispersed phase [15, 29]. Within literature, there are two competing notions concerning the influence of concentration and shear rate on the rheological properties of fluids. To determine whether a fluid exhibits Newtonian or non-Newtonian behaviour, one examines the relationship between the shear stress and shear rate that is usually presented using the Ostwald formula [79]:

$$\tau = K\dot{\gamma}^{(n-1)} \quad (8)$$

where  $n$  is the fluid behaviour index and describes the degree of non-Newtonian behaviour exhibited and  $K$  is the consistency index, where the larger the value of  $K$ , the more viscous the fluid is. A value of  $n = 1$  indicates Newtonian behaviour,  $n > 1$  shear-thickening behaviour and  $n < 1$  shear-thinning behaviour. Morimoto and Kumano [15] defined  $n$  experimentally and found that after melting the dispersions displayed Newtonian behaviour with  $n = 0.95$ , which was attributed to the liquid state of the particles becoming more deformable which created a more Newtonian behaviour. The first competing notion in literature, is that at and below a 30 wt.% of dispersed phase, PCD demonstrate Newtonian behaviour, and above this concentration non-Newtonian behaviour is observed [62]. Vasile et al. [50] investigated the rheology of a 30 wt.% paraffin-in-water emulsion and found that the emulsion exhibited Newtonian behaviour with measurements performed on a rheometer in both the cone and plate geometry. Morimoto et al. [15] discovered that dispersions with 10-30 wt.% paraffin were considered to be Newtonian, whereas a dispersion containing 40 wt.% paraffin was considered non-Newtonian. This was attributed to higher concentrations of dispersed phase having a greater probability of generating aggregation-type structures, which cause more non-Newtonian behaviours. Chen et al. [27] also found that the friction factor of the 30 wt.% conformed to the classical formula of [27]:

$$f = \frac{64}{Re} \quad (9)$$

for laminar flow in circular pipes which confirmed its Newtonian behaviour. Conversely, the second notion is that all concentrations of paraffins show non-Newtonian behaviour. Huang et al. [33] investigated a larger range of paraffin concentrations, 15-75 wt.% and discovered that they all exhibited non-Newtonian behaviour and that the degree of non-Newtonian behaviour and viscosity dramatically increased once the paraffin concentration surpassed 50 wt.%. In another investigation by Huang et al. [29] dispersions containing RT10 with weight percentages of 15 to 50% all exhibited non-Newtonian behaviour. Lu and Tassou [30] also found that non-Newtonian behaviour was observed for a dispersion of 30 wt.% RT6 and a dispersions of 6 wt.% RT25. The conflict in these findings can be attributed to other factors that contribute to the rheology of dispersions such as surfactant type and concentration, temperature and shear rate.

### 3.5.2. Effect of surfactant choice

The role the surfactant plays in influencing the viscosity of PCD is attributed to the micelle structure, which is formed by the surfactant interface. This indicates that the viscosity is dependent on both the surfactant type and their respective concentrations. Zhang et al. [40] investigated the effects of three commonly used surfactants, SDS, Tween 80 and Tween 20 on the viscosity of a 30 wt.% hexadecane dispersion. It was concluded that there was great variation in the viscosities by just changing the type of surfactant used. Zhao and Shi [78] built on the idea of the surfactant influence by investigating the effect of the surfactant concentration on the viscosity. The surfactant concentration was varied from 2.6 to 4.7 wt.% and a corresponding dynamic viscosity change of 0.00055 Pa·s to 0.00294 Pa·s was observed at 20 °C. This can be explained by recognising that as the surfactant concentration increases, there will be an increased attraction strength of the surfactant monolayer. This increased attraction requires more energy to be transported than a smaller attraction strength, thus increasing the viscosity [78]. It is suggested by the authors that due to the complex surfactant system now employed in dispersions, as seen in the previous section, with co-surfactants and using a variety of surfactants mixed together that rheological properties are properly understood and tested for multi-component dispersion compositions.



### 3.5.3. Effect of temperature

Lu and Tassou [30] discovered that the viscosity of their PCD was heavily dependent on the temperature, where a decrease in temperature led to an increase in viscosity until the crystallisation temperature was reached. This was attributed to the presence of surfactants, as the liquid paraffin droplets remain smooth and flexible until their crystallisation point and therefore make little contribution to the friction. This was also confirmed by Huang et al. [24] who discovered that the viscosity of all the tested dispersions increased with the increasing frozen fraction of the RT10 paraffin in the dispersion, therefore as the temperature decreased the viscosity increased. This has been attributed to the fact that solid particles are less likely to deform under shear stress like liquid droplets, therefore increasing the viscosity. The variation of the viscosity with temperature was also found to be reduced for dispersions with lower paraffin concentrations, caused by the difference in water content [50]. Chen et al. [27] revealed that viscosities decrease with an increase in temperature, and the larger the mass fraction of the PCD, the quicker this effect is observed. For example, at 0 °C the viscosity of a 30 wt.% hexadecane dispersion was 42 mPa·s and at 30 °C was 17 mPa·s, whereas the 10 wt.% hexadecane dispersion had a viscosity of 4 mPa·s at 0 °C and 2 mPa·s at 30 °C. The temperature dependency of viscosity is due to the tendency of droplets to aggregate at lower temperatures, as explained by Zhang et al [40]. Zhang et al. [40] performed further experimentation on a capric/lauric acid-in-water dispersion and found that the cohesion of PCM droplets influenced the viscosity. This was attributed to temperature increases causing an increased distance between the PCM droplets thus reducing the attractive forces holding them together. In turn, this reduces the shear stress by deformation and therefore a reduced viscosity is shown

### 3.6. Physical properties summary

It is evident to see that all the aforementioned physical properties of PCD; stability (during cycling and storage), degree of supercooling, heat capacity, thermal conductivity and viscosity are influenced by the formulation and physical and operational parameters and conditions used when creating and testing PCD. These parameters include the concentration of PCM used, the effect of temperature, the effect of PCM droplet size and the effect of chemical additives. It is important to understand the dual-nature that some of these parameters and conditions have on the physical properties of PCD for future optimisation of PCD formulations and to glean information on how these parameters can be balanced to create a HTF which fulfils the requirements outlined in Section 3. Additionally, the hysteresis between the cooling and heating cycles of such behaviour is poorly reported, and the authors believe a thorough investigation into the thermal cycling of all physical properties should be conducted.

## 4. Heat transfer

Unlike microencapsulated phase change slurries, limited investigations, both experimentally and numerically have been performed on PCD. Experimental studies for PCD as potential HTF are essential as they not only have the potential to demonstrate the benefits of using PCD, but also they help to understand the heat transfer processes and mechanisms that occur in PCD. Ultimately, this allows predictive correlations to be produced for heat exchanger design and optimisation. The phase change process of PCD occurs over a temperature range where the PCD has a much higher specific heat capacity (during phase change) than a single-phase fluid. This means that a PCD has a much larger ability to transport heat. Zhao and Shi [78] provide a theoretical analysis of this and found that convective heat transfer can be increased if the flow rate of the fluid is increased, the temperature gradient is increased and certain material properties, such as the specific heat is increased.

This section on heat transfer will be separated into the different operational parameters that can be controlled when performing experiments with PCD. Ma et al. [35] explained the physical reason for the influence of physical operational parameters on the melting heat transfer performance of PCD. The author stated that during melting, a liquid layer of melting PCM droplets near the tube wall impedes the heat transfer from the wall to the bulk of the fluid. This effectively reduces the heat transfer from the wall to the bulk, and certain operational parameters such as the flow rate, imposed temperature or heat flux at the wall and mass concentration of PCM effect the rate at which this liquid layer develops. [35]. This is discussed further in section 4.1.

Furthermore, for implementation of PCD into industrial and commercial systems, a complete understanding of both the melting and crystallisation heat transfer behaviour is required to understand the complete cycle of PCD. Therefore, in this section the effect of the operational parameters are further split into melting and crystallisation experiments. Additionally, forced convection is more highly studied than natural convection, due to the usefulness of forced convection in temperature stability and refrigeration applications and this is the focus of this review. Despite

578 this, natural convection is still the focus of a few research articles, where the motivation is energy storage owing to the  
579 latent heat of phase change for PCD [76, 80].

## 580 4.1. Melting

581 Generally, authors focus their heat transfer experiments on the melting behaviour of PCD because during crystalli-  
582 sation the supercooling phenomena makes the heat transfer behaviour difficult to predict.

### 583 4.1.1. Effect of the wall heat flux

584 Morimoto and Kumano [15] found that a higher applied wall heat flux decreased the local heat transfer coefficient  
585 due to a faster melting PCD. Ma et al. [35] explained this by stating that the mass fraction of un-melted PCM is larger  
586 at lower heating powers at the same axial location as higher heating powers and therefore the liquid layer of melted  
587 PCM, which usually hinders heat transfer develops slower at lower heat fluxes. Ho et al. [6] varied the heat flux in  
588 their divergent mini-channels and found that with PCD, when the wall heat flux was decreased that the dimensionless  
589 wall temperature would also decrease, suggesting a greater degree of melting. However, Ho et al. [6] discovered that  
590 the heat flux had a minor effect on the average Nusselt number ( $Nu$ ). Morimoto and Kumano [15] showed that the  
591 enhancement ratio of  $Nu$  (of the PCD to the base fluid) was decreased as the wall heat flux was increased. This was  
592 most likely due to the latent heat absorption decreasing as the wall heat flux increased. This effect was shown through  
593 the following relation for the modified specific heat capacity ( $c_p^*$ ) inside the thermal boundary layer MORIMOTO2018:

$$c_p^* \approx c_p + \frac{L}{(T_w - T_{in})} \quad (10)$$

594 where  $L$  is the latent heat of melting for the PCD,  $T_w$  is the wall temperature and  $T_{in}$  is the bulk inlet flow temperature.  
595 From Equation 10 when a low heat flux is applied, almost all the heat is allocated to the latent heat of the PCM because  
596 the temperature difference between the main flow and the wall temperature is relatively small. On the other hand,  
597 when a relatively high wall heat flux is applied, the heat is transferred under the form of sensible heat because the wall  
598 temperature is relatively high and the temperature of the PCD increases even though the PCM particles are melting.  
599 This was also validated with numerical results [15].

### 600 4.1.2. Effect of the mass flow rate

601 It is important to note that in all experimental and numerical investigations on the heat transfer of PCD, the flow  
602 regime is always described as turbulent or laminar, which is a classification generally attributed to single-phase fluids,  
603 such as water. However, for PCD, laminar and turbulent flow regimes are more difficult to define without a set of  
604 standard PCD formulations (including set droplet sizes and PCM concentrations) and there is little discussion on the  
605 validity of describing PCD as flowing in the turbulent or laminar flow regime, especially when they have a non-  
606 Newtonian behaviour: the laminar turbulent transition of such fluids remains a non fully solved scientific issue.

607 Ho et al. [6] found that when a higher mass flow rate was used, the dimensionless wall temperature increased  
608 because the effective heat exchange duration between the PCD and the wall was too short. However, this occurs at  
609 a critical Reynolds number ( $Re$ ) and generally, an increase in  $Re$  number in the turbulent flow regime increases the  
610 heat transfer behaviour. Ho et al. [6] found that an increase in  $Re$  number increased the average  $Nu$  due to thinning  
611 of the thermal boundary layer resulting in an increased heat transfer rate. Ma et al. [35] also stated that an increase  
612 in  $Re$  increased the local heat transfer coefficients due to greater thinning of the thermal boundary layer. Morimoto  
613 and Kumano [81] suggested that the thermal boundary layer development was suppressed largely at higher flow rates,  
614 attributing to higher heat transfer coefficients. Despite this, Roy and Avanic [82] numerically found that in the laminar  
615 flow regime, the dimensionless wall temperature was independent of the  $Re$  used for their octadecane-in-water PCD.  
616 This is what is observed for single-phase fluids, such as water and further indicates the need for more research in  
617 attributing PCD to the turbulent or laminar flow regime. Saarinen et al. [49] discovered similar results in the turbulent  
618 regime where for  $Re = 2300-6000$ ,  $Nu$  enhancement did not increase a great deal. However, at  $Re = 7000$ , the highest  
619  $Nu$  enhancements of 13-15% were obtained. Additionally, the same results could be seen for the convective heat  
620 transfer coefficients. Therefore,  $Re = 7000$  was classified as a critical  $Re$  by the authors [49].

### 621 4.1.3. Effect of the PCM concentration

622 Cho et al. [83] numerically investigated a PCD in a mini-channel and found that increasing the concentration of the  
623 PCM in the PCD decreased the wall temperature increase along the channel compared to the base fluid. Cho et al. [83]



624 attributed this to an increased melting time of the PCM when the concentration of the PCM is higher. Furthermore,  
625 Morimoto and Kumano [15] numerically investigated the heat transfer behaviour of a PCD, in laminar flow, and found  
626 that the numerically obtained  $Nu$  agreed with the experimentally obtained results for 20 and 30 wt.% PCM based PCD.  
627 However, the numerical model showed much lower values for Nusselt at 10 wt.% than the experimental results, they  
628 concluded that heat transfer promotion mechanisms occurred in PCD with low PCM concentrations. Ma et al. [35]  
629 found that the local heat transfer coefficient increased with the mass concentration of PCM used whereby the local heat  
630 transfer coefficient of a 20 wt.% PCM dispersion was found to be 1.4 times higher than a 10 wt.% PCM dispersion at  
631 the same Reynolds. Overall, despite the increase in the heat transfer performance with an increase in the concentration  
632 of PCM (at the same  $Re$ ), a compromise of the mass fractions of PCM used in PCD needs to be found by weighing up  
633 the increase in thermal performance and the additional increase in viscosity and pumping power required. This is  
634 discussed further in section 5.

#### 635 4.1.4. Other notable effects

636 Wen and Ding [84] numerically found that during melting, a non-uniform particle size distribution resulted in  
637 higher Nusselt numbers because of particle migration and Brownian motion. During melting, Ma et al. [35] found that  
638 although the development of the thermal boundary layer is faster in smaller tubes than in larger tubes that the Nusselt  
639 number increased in smaller tubes. This was attributed to greater particle-wall interactions in smaller tubes.

## 640 4.2. Crystallisation

641 To date, very few studies have been performed examining the heat transfer behaviour during crystallisation. As  
642 aforementioned, the supercooling makes analysis and creating correlations more difficult.

### 643 4.2.1. Effect of the flow regime

644 Morimoto et al. [37] found that a turbulent flow regime caused an increase in the heat transfer promotion effect.  
645 Despite Roy and Avanic [82] finding that during melting the heat transfer coefficient was independent of the Reynolds  
646 number in laminar flow, Vasile et al. [50] discovered that the average heat transfer coefficient increased as the  $Re$   
647 increase in a laminar flow regime for crystallisation.

### 648 4.2.2. Effect of the PCM concentration

649 Zhao and Shi [78] discovered that in a coiled circular tube that  $Nu$  increased as the mass fraction of the PCM was  
650 increased. Inaba and Morita [77] experimentally investigated a tetradecane-in-water PCD in a double-tube coiled heat  
651 exchanger and showed that an increase in the concentration of the PCM in the PCD led to an increase in the  $Nu$ .

### 652 4.2.3. Other notable effects

653 Alongside the main operational parameters, several other parameters have been noticed to affect the heat transfer  
654 behaviour of PCD. Inaba and Morita [77] stated that a decrease in the temperature difference between the PCD and  
655 the fluid cooling it down increases the heat transfer performance of the PCD. Zhao and Shi [78] found that the Nusselt  
656 number for the solid dispersed phase (after phase change) was larger than for the liquid dispersed phase (before phase  
657 change). The two explanations which were presented are, firstly that the emulsion becomes a solid-liquid two phase  
658 fluid when the emulsion temperature falls below the freezing point and the mixing and disturbing effects caused by small  
659 particles improve the convective heat transfer in the thermal boundary layer. Secondly, the emulsion's effective thermal  
660 conductivity has a somewhat higher value when the dispersed phase becomes solid particles. Inaba and Morita [77] also  
661 found that for the solidified PCM a larger Nusselt enhancement was obtained due to the higher thermal conductivities  
662 in the solid phase. Morimoto et al. [37] investigated two different PCD with different surfactants, they plotted the  
663 Nusselt number for each PCD versus the dimensionless cooling distance alongside the Dittus–Boelter equation (from  
664 [37] for a single-phase fluid, as shown in Figure 7. From Figure 7, the initiation of solidification time is different for  
665 each different surfactant used and the deviation between the empirical equation for a single-phase fluid and the Nusselt  
666 number's experimentally observed are greater for the PCD with Tween 60 surfactant than Tween 80 surfactant. This  
667 deviation suggests that surfactants can also play a role in the heat transfer performance of PCD during crystallisation  
668 and this is something which needs to be further researched.

## 669 4.3. Heat transfer summary

670 Overall, the lack of experiments, both numerically and experimentally can be seen for crystallisation of PCD. This  
671 creates a problem because in all usages of PCD, knowledge of the full melting-crystallisation cycle is needed to design

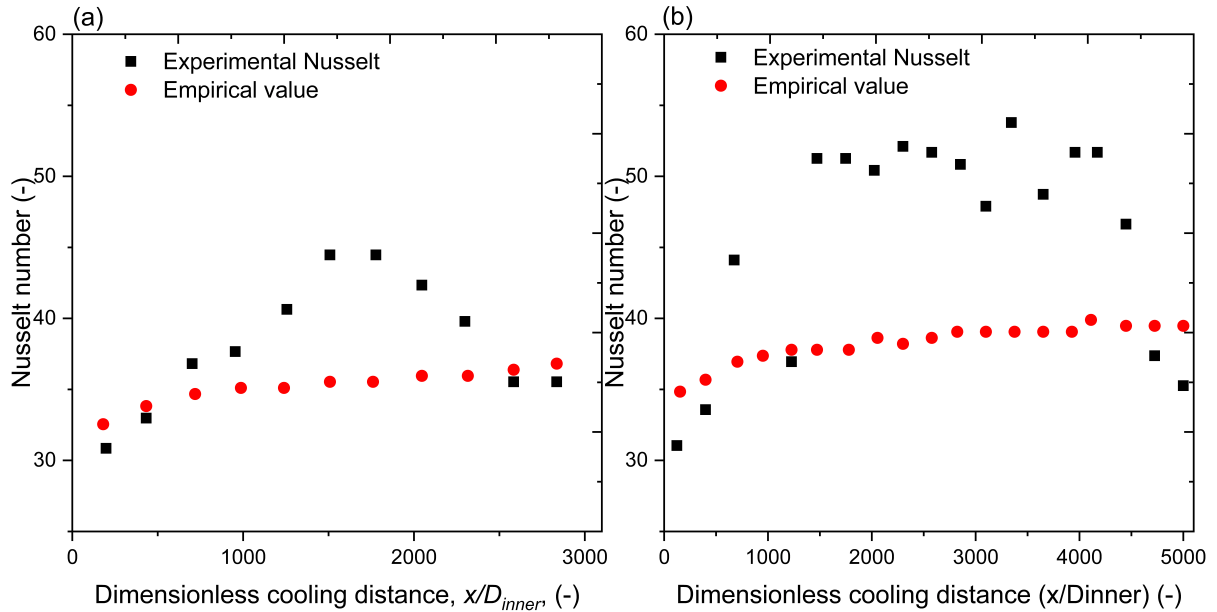


**Figure 7:** The local Nusselt number versus the dimensionless distance from inlet and the empirical correlation for single-phase fluid for (a) a PCD with Tween 80 as the surfactant and for (b) a PCD with Tween 60 as the surfactant. Figure was adapted from Morimoto et al. [15].

672 and optimise systems. Additionally, there are generally few research articles published on the heat transfer behaviour of  
 673 PCD, and few standardised methods of experimentation, due to different geometries and boundary conditions chosen  
 674 for experiments. It is also acknowledged by the authors that due to the lack of research on defining and validating flow  
 675 regimes as laminar or turbulent in the case of PCD that the transition flow regime remains a non fully solved scientific  
 676 issue and the heat transfer performance during this transition is unknown. Overall, this makes having a comprehensive  
 677 understanding of the heat transfer and the factors which affect the heat transfer performance of PCD very difficult,  
 678 especially when studies focus primarily on the melting and few correlations exist describing the heat transfer during  
 679 crystallisation.

## 680 5. Figures of merit

681 To choose the appropriate PCD for a specific application, the heat transfer capabilities of the dispersion compared  
 682 to its base fluid or the standard HTF must be calculated. Figures of merits aim to characterise this comparison and  
 683 comparison criteria are used to set the conditions under which the figure of merit comparison takes place. Additionally,  
 684 an important aspect of experimental research into PCD is to produce predictive equations for heat transfer coefficients,  
 685 which eventually permits the effective design of heat exchangers and pipe geometries. For these equations to be  
 686 applied to real applications, non-dimensional parameters are used to represent heat transfer coefficients, thermophysical  
 687 properties and geometric configurations. For heat transfer fluids, the most commonly used dimensionless numbers are  
 688 Nusselt, Prandtl ( $Pr$ ) and Reynolds. When choosing an appropriate PCD, there are three main parameters, which are  
 689 of the upmost importance; these are highlighted at each point of the triangle in Figure 8. Firstly, the heat transfer  
 690 coefficient,  $h$ , this is a direct measurement of the heat transfer performance of a fluid and is thus vital in the generation  
 691 of a figure of merit for PCD performance characterisation. Secondly, the pressure drop,  $\Delta p$ , which increases due to the  
 692 increased viscosity of the phase change of the PCD and impairs the applicability of PCD. Finally, the capacity flow  
 693 rate, which is taken into account because of the increase in specific heat capacity of the PCD during phase change.  
 694 The figures of merit found in literature are colour coded with the respective operational parameters that they take into  
 695 consideration in Figure 8.

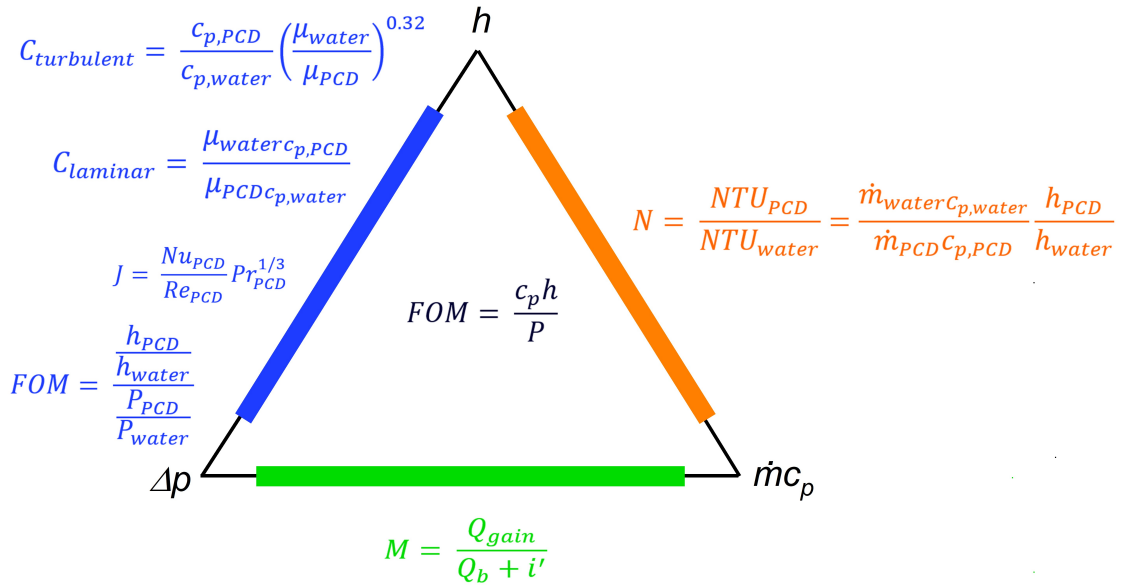


Figure 8: A depiction of the three key parameters for PCD comparison and their respective figures of merit

### 5.1. Comparison criteria

Within literature, the most frequently used comparison criteria are  $Re$ , flow velocity and pumping power. Whilst  $Re$  number is often used as a comparison criterion, it is generally an inappropriate choice because comparison under the same  $Re$  suggests that the flow velocity for the less viscous base fluid (water) is lower than for the more viscous PCD, which indicates that under the constant  $Re$  comparison criterion the observed effect is a mixture of both the flow velocity effects and the thermophysical properties of the PCD and base fluid respectively [70]. Additionally, constant  $Re$  for comparison omits the increase in pumping power required with a more viscous PCD which is pumped at a higher flow velocity to reach the same  $Re$  as the less viscous base fluid. However, under the constant flow velocity comparison criterion, the flow velocity effect, which is inherently present under the constant  $Re$  comparison criterion, is eliminated. A PCD with the same velocity (or mass flow) as the base fluid will have a larger specific heat capacity flow due to the available latent heat [70]. Temperature increase will be lower and driving temperature difference higher, which results in larger heat transfers even though the heat transfer coefficient might be smaller. Even though the pumping power for PCD is higher than for the base fluid, it has been found that in many applications the pumping power difference between a PCD and its base fluid is small at the same flow velocity. Furthermore, the constant pumping power comparison, which compares the heat transfer under the condition that the PCD and base fluid require the same amount of pumping power suggests that the flow velocity for the more viscous PCD is slightly lower than for the base fluid [70]. However, the constant pumping power comparison criteria represents the most explicit choice of criteria and should be used when the relevant information is known.

### 5.2. Nusselt number based figures of merit

$Nu$  is a dimensionless form of the heat transfer coefficient that should be used to depict the convective heat transfer performance of HTF. Bonjour et al. [85] used the Colborn Factor ( $J$ ), to assess the heat transfer versus the necessary pressure drop for a specific flow where  $J$  is defined as follows:

$$J = \frac{Nu_{PCD}}{Re_{PCD} Pr_{PCD}^{1/3}} \quad (11)$$

It is useful because it shows the dependency of heat exchange on  $Re$  and therefore the optimal surface depends on the  $Re$  of interest and thus the Colburn Factor.  $Nu$  can be interpreted as the ratio between the convective heat transfer (including advection and diffusion) to the conductive heat transfer within a fluid.  $Nu$  is useful in defining the heat transfer mechanisms which occur in the PCD.

### 5.3. Heat transfer coefficient based figures of merit

Oftentimes the figure of merit of comparing heat transfer coefficients, is referred to the heat transfer effectiveness and is defined as the ratio of the convective heat transfer coefficient for the PCD relative to the convective heat transfer coefficient of the base fluid as below [84, 86]:

$$\epsilon = \frac{h_{PCD}}{h_{water}} \quad (12)$$

where  $h_{PCD}$  and  $h_{water}$  are the heat transfer coefficients for the PCD and the base fluid (water) respectively at the same mass flow rate. From this, an enhanced heat transfer ability of the PCD is observed when  $\epsilon > 1$ . Memon et al. [87] investigated different PCD by using the heat transfer effectiveness ratio, and found that the maximum ratio was reached when all the particles of the PCM were melted inside the dispersion. It was further concluded that this ratio could be further enhanced by minimising the sensible heat region at the inlet of the flow channel, which would allow the remaining length of the channel to be represented by the latent heat effect. In turn, this would permit a lower temperature increase along the channel and a greater temperature control within the channel. This can be shown non-dimensionally in the form of the Stefan number ( $Ste$ ), which represents the ratio of the sensible heat to latent heat as shown in Equation 13.

$$Ste = \frac{C_p \Delta T}{L} \quad (13)$$

for the boundary condition of constant wall temperature or defined as [16]:

$$Ste = \frac{c_p(q/\lambda)}{\psi L_{PCM}} \quad (14)$$

For the boundary condition of constant wall heat flux. The Stefan number has been used in some investigations to determine the melting time. Morimoto et al. [81] used a modified Stefan number and discovered that the Nusselt number increases when the modified Stefan number decreased meaning that the Nusselt number was found to increase when the heat allocated to the latent heat of phase change increased. Ma et al. [35] also used the Stefan number to investigate the optimal heat input to use to obtain the best heat transfer performance of their PCD.

Ho et al. [86] went further and discussed the dependence of  $\epsilon$  on  $Re$  and found a critical velocity to enhance  $\epsilon$ . At extremely high  $Re$ , the sensible heat dominates over the latent heat of the PCD due to the particles only partially melting due to higher flow velocity, whereas at slightly lower  $Re$ , the PCM particles within the slurry have more time to absorb the surrounding heat and are therefore more likely to fully melt. It is suspected by Memon et al. [87] that the maximum value of the effectiveness ratio is obtained when the sensible region at the inlet is minimised, and that the peak in effectiveness ratio is when the flow through the length of the channel is dominated by latent heat of phase change of the PCM. Further investigation into this by use of  $Ste$  is recommended by the author for future research.

### 5.4. Pumping power based figures of merit

Whilst an increase in the heat transfer coefficient is advantageous for PCD, an increase in the pumping power is detrimental for their use as HTF. As a result of this, the two quantities can be combined to form a new figure of merit which shows the ratio of the heat transfer coefficient increase to the pumping power enhancement and is defined as [70]:

$$FOM = \frac{h_{PCD}/h_{water}}{P_{PCD}/P_{water}} \quad (15)$$

If this figure of merit is utilised under the constant pumping power comparison criterion, then it reduces to the ratio of heat transfer coefficients between the PCD and the base fluid, see Equation 12. When the figure of merit is higher, it is indicative that there is a greater heat transfer increase when using the PCD than pumping power penalty.

Memon et al. [87] defined a figure of merit based on the pumping power and heat transfer named Merit number ( $M$ ). It uses a measure of the irreversibility of the heat transfer and frictional losses due to the addition of the PCM particles within a fluid. Subsequently, it represents the ratio of the enhancement in heat transfer due to PCM addition to the total of the heat transfer to the top wall of the channel and the irreversibility.  $M$  is defined as:

$$M = \frac{Q_{gain}}{Q_b + i'} \quad (16)$$

760 where  $Q_{gain}$  is the rate of increase of heat absorption in the dispersion due to the addition of the PCM,  $Q_b$  is the heat  
 761 transfer rate of the bulk fluid to the wall and  $i'$  is the rate of irreversibility the definitions of both can be found in [87].  
 762 The irreversibility depends on the volumetric entropy generation rate which is defined in [88]. It is expected that at  
 763 higher heat flux to mass ratios, the lower concentration of dispersions will show higher  $M$  values, this is suspected  
 764 because the heat transfer enhancement is smaller than the increase in irreversibility, due to higher pressure-drops and  
 765 viscosities.

### 766 5.5. Heat capacity based figures of merit

767 In laminar flow regimes, Prasher et al. [89] suggested the following F.O.M. ratio [89]:

$$\frac{C_\mu}{C_\lambda} = \frac{\frac{\mu_{PCD} - \mu_{water}}{\mu_{water}}}{\frac{\lambda_{PCD} - \lambda_{water}}{\lambda_{water}}} \quad (17)$$

768 where it was stated that for  $\frac{C_\mu}{C_\lambda} < 4$ , the PCD is considered better in terms of the heat transfer compared to the base  
 769 fluid (water). Fischer et al. [56] also investigated this figure of merit, and named it the heat capacity rate ratio,  $C$ . This  
 770 can be seen in Equation 2. The derivation for  $C$  can be seen in [56]. It was discussed that  $C$  cannot be applied directly  
 771 to turbulent flow. This is because the derivation of this equation involves calculating the pressure drop in the pipe, and  
 772 then equating the pressure drop of water and PCD. This is possible in laminar flow, however due to the exponent in the  
 773 pressure drop calculation in a pipe for turbulent flow this cannot be equated.

### 774 5.6. Figures of merit summary

775 Overall, the heat transfer and rheological performance of new HTF need to be compared to the heat transfer perfor-  
 776 mance of existing HTF. For choosing an appropriate HTF, the three main parameters which need to be considered are  
 777 the heat transfer coefficient, the pressure drop and the capacity flow rate. As discussed in Sections 3 and 4, there are  
 778 many factors which need to be considered when formulating and using PCD as an enhanced HTF. Figures of merit aim  
 779 to quantify these parameters and allow a direct comparison between different HTF on their performance for specific  
 780 applications under certain comparison criteria.

## 781 6. Conclusions and Future directions

782 This review has focused on and highlighted the types of PCD that have been investigated in the literature, along-  
 783 side their thermophysical, rheological and heat transfer properties. It clearly demonstrates that the increased heat  
 784 capacities shown by dispersions renders them strong candidates for HTF. The thermophysical properties of paraffins  
 785 as phase change material in dispersions are widely reported for a broad temperature range within the cooling domain;  
 786 however, low thermal conductivities indicate that other classes of materials should be investigated to increase the heat  
 787 transfer capabilities. Currently, the application of PCD into systems for cooling has been limited on accounts of large  
 788 degrees of supercooling of dispersions because of their microscopic geometries and stability observed both in stor-  
 789 age and during cycling. Additionally, from this review, it has been highlighted that out of the functional latent heat  
 790 transfer fluids developed, phase change dispersions are the least investigated, particularly in terms of heat transfer  
 791 and the mechanisms of heat transfer. Whilst numerical models have been developed in both laminar and turbulent  
 792 flow, experimental validation is still required. It has been suggested that for PCD to become prevalent as heat transfer  
 793 fluids, a more comprehensive understanding and validation of their heat transfer performance is required. This is in  
 794 order to design correct heat exchangers and optimise the cooling system geometries. Additionally, the heat transfer  
 795 performance of PCD undergoing crystallisation needs more attention than melting due to the lack of studies performed  
 796 during solidification. On top of this, an effective model to describe the rheology of dispersions should be generated as  
 797 currently literature offers conflicting experimental results, most likely due to different test set-ups and data collection  
 798 methods. Furthermore, this review highlights the need to be careful in designing PCD for cooling applications, due to  
 799 the positive and negatives effects each parameter can have on the PCD as a fluid overall. An overview of the different  
 800 formulation properties and controlled parameters; PCM concentration, surfactant system, temperature, droplet size,  
 801 chemical additives, wall heat flux and mass flow rate on the PCD properties and behaviour; stability, supercooling,  
 802 heat capacity, thermal conductivity, viscosity and heat transfer performance are given in Table 3.

803

804 Whilst the current standard PCM used in PCD is paraffins, as can be seen by Tables 1 and 2, the global standards  
805 for improving sustainability amongst energy solutions will encourage researchers to investigate bio-based PCM for  
806 use in PCD, such as fatty acids and esters. New PCMs will require new literature in terms of formulation such as;  
807 effective surfactant systems and nucleating agents. One of the main future directions of the formulation of PCD, will  
808 be more attention given to the finding of novel and efficient nucleating agents, and testing whether these nucleating  
809 agents hold up over thermo-mechanical cycling and storage. Particularly, the use of surfactants to initiate nucleation  
810 (reduce supercooling) will be a future direction of PCD formulation research. Once a greater understanding of the  
811 interfacial tension, and crystallisation kinetics of phase change dispersions has been achieved, and more research has  
812 been performed, carefully selecting surfactant systems to induce nucleation will become more commonplace when  
813 formulating PCD. Additionally, this balance between choosing the appropriate surfactant system for stability and for  
814 inducing nucleation will have to also be investigated. Furthermore, once supercooling has been successfully reduced  
815 within phase change dispersions, more attention should be geared towards investigating the heat transfer behaviour of  
816 PCD during crystallisation and the author's believe that as more PCD are pushed into the developmental stage, that  
817 more research will focus on crystallisation as a complete understanding of the heating-melting cycle will need to be  
818 considered for implementation into cooling systems.

**Table 3**  
**Overview of the formulation properties and controlled parameters on the thermophysical and heat transfer behaviour of PCD**

Controlled Parameters	PCD Properties and behaviour						
	Stability	Supercooling	Heat Capacity	Thermal Conductivity	Viscosity	Heat transfer coefficient and Nusselt number	
PCM concentration	Higher PCM concentrations increase storage stability	-	Higher PCM concentrations increase the heat capacity	Higher PCM concentrations decrease the thermal conductivity of the PCD	High PCM concentrations increases viscosity	Increased PCM concentrations increases the Nu and h during melting and crystallisation	
Effect of surfactant used	Surfactant HLB of 12.0 optimum for stability	Different surfactants affect the degree of supercooling of PCD. heptadecanol as a co-surfactant has been showed to reduce the supercooling degree.	-	-	Different surfactants change the micelle structure of the PCM droplets and thus the viscosity. Increasing surfactant concentrations increases the viscosity of PCD.	During crystallisation, due to the effect of surfactants on crystallisation temperature, certain surfactants have also been shown to increase the Nu	
Effect of temperature/phase change	Higher stabilities when PCM is crystallised	-	-	After the PCM has melted the thermal conductivity decreases	Decrease in temperature leads to an increase in the viscosity. When the PCM is crystallised, the viscosity is increased.	PCD with crystallised PCM had higher Nu than PCD with liquid PCM	
PCM droplet size	Narrower particle size distributions increase stability	Smaller particle sizes increase the degree of supercooling	-	A smaller PCM droplet size increases the thermal conductivity of PCD	-	Non-uniform droplet sizes resulted in higher Nu during melting	
Effect of additives	Silicon dioxide nanoparticles have been found to increase the stability	Nucleating agents such as higher melting point paraffins, MCNT have been effective in reducing the supercooling.	Additives reduce the amount of PCM used and thus decrease the heat capacity of PCD	Aluminium nanoparticles have been shown to increase the thermal conductivity of PCD	-	-	
Effect of wall heat flux	-	-	-	-	-	During melting, when the wall heat flux is too high, the Nu was found to decrease	
Effect of mass flow rate	-	-	-	-	-	During crystallisation, an increase in the mass flow rate was found to increase the Nu. However, during melting a critical Reynolds was found. When a Reynolds above the critical value was found a high Nusselt enhancement was obtained.	

## References

- 819
- 820 [1] Paris IEA. The future of cooling.
- 821 [2] M. Caliano, N. Bianco, G. Graditi, and L. Mongibello. Analysis of a phase change material-based unit and of an aluminum foam/phase change  
822 material composite-based unit for cold thermal energy storage by numerical simulation. *Appl. Energy*, 256:113921, 2019.
- 823 [3] T. Yang, C. Wang, Q. Sun, W. Qie, and W. Ronald. Study on the application of latent heat cold storage in a refrigerated warehouse. *Energy*  
824 *Procedia*, 142:3546–3552, 2017.
- 825 [4] X. Xu, X. Zhang, and S. Liu. Experimental study on cold storage box with nanocomposite phase change material and vacuum insulation panel.  
826 *Int. J. Energy Res.*, 42(14):4429–4438, 2018.
- 827 [5] J. Chen and P. Zhang. Preparation and characterization of nano-sized phase change emulsions as thermal energy storage and transport media.  
828 *Appl. Energy*, 190:868–879, 2017.
- 829 [6] C. Ho, C. Huang, C. Qin, and w. Yan. Thermal performance of phase change nano-emulsion in a rectangular minichannel with wall conduction  
830 effect. *Int. Commun. Heat Mass Transf.*, 110:104438, 2020.
- 831 [7] F. Wang, J. Cao, Z. Ling, Z. Zhang, and X. Fang. Experimental and simulative investigations on a phase change material nano-emulsion-based  
832 liquid cooling thermal management system for a lithium-ion battery pack. *Energy*, 207:118215, 2020.
- 833 [8] L. Fischer, S. von Arx, U. Wechsler, S. Züst, and J. Worlitschek. Phase change dispersion properties, modeling apparent heat capacity. *Int. J.*  
834 *Refrig.*, 74:240–253, 2017.
- 835 [9] S. Shibusatani. Pcm-micro capsule slurry thermal storage system for cooling in narita airport. *Proc. 3rd Expert. Meet. Work. IEA Annex 17.*,  
836 *IEA,Lublijana*, 2002:118215, 2020.
- 837 [10] G. Zhang, Z. Yu, G. Cui, B. Dou, W. Lu, and X. Yan. Fabrication of a novel nano phase change material emulsion with low supercooling and  
838 enhanced thermal conductivity. *Renewable Energy*, 151:542–550, 2020.
- 839 [11] F. Wang, X. Fang, and Z. Zhang. Preparation of phase change material emulsions with good stability and little supercooling by using a mixed  
840 polymeric emulsifier for thermal energy storage. *Sol. Energy Mater Sol. Cells*, 176:381–390, 2018.
- 841 [12] E. Shchukina, M. Graham, Z. Zheng, and D. Shchukin. Nanoencapsulation of phase change materials for advanced thermal energy storage  
842 systems. *Chem. Soc. Rev.*, 47(11):4156–4175, 2018.
- 843 [13] D. McClements. Nanoemulsions versus microemulsions: terminology, differences, and similarities. *Soft matter*, 8(6):1719–1729, 2012.
- 844 [14] T. Kawanami, K. Togashi, K. Fumoto, S. Hirano, P. Zhang, K. Shirai, and S. Hirasawa. Thermophysical properties and thermal characteristics  
845 of phase change emulsion for thermal energy storage media. *Energy*, 117:562–568, 2016.
- 846 [15] T. Morimoto and H. Kumano. Flow and heat transfer characteristics of phase change emulsions in a circular tube: Part 1. laminar flow. *Int. J.*  
847 *Heat Mass Transf.*, 117:887–895, 2018.
- 848 [16] Q. Li, G. Qiao, E. Mura, C. Li, L. Fischer, and Y. Ding. Experimental and numerical studies of a fatty acid based phase change dispersion for  
849 enhancing cooling of high voltage electrical devices. *Energy*, 198:117280, 2020.
- 850 [17] L. Chai, R. Shaukat, L. Wang, and H Wang. A review on heat transfer and hydrodynamic characteristics of nano/microencapsulated phase  
851 change slurry (n/mpcs) in mini/microchannel heat sinks. *Appl. Therm. Eng.*, 135:334–349, 2018.
- 852 [18] Z. Qiu, X. Ma, P. Li, X. Zhao, and A. Wright. Micro-encapsulated phase change material (mpcm) slurries: Characterization and building  
853 applications. *Renew. Sustain. Energy Rev.*, 77:246–262, 2017.
- 854 [19] M. Delgado, A. Lázaro, J. Mazo, and B. Zalba. Review on phase change material emulsions and microencapsulated phase change material  
855 slurries: materials, heat transfer studies and applications. *Renew. Sustain. Energy Rev.*, 16(1):253–273, 2012.
- 856 [20] M. Jurkowska and I. Szczygieł. Review on properties of microencapsulated phase change materials slurries (mpcms). *Appl. Therm. Eng.*,  
857 98:365–373, 2016.
- 858 [21] Z. Chen and G. Fang. Preparation and heat transfer characteristics of microencapsulated phase change material slurry: a review. *Renew.*  
859 *Sustain. Energy Rev.*, 15(9):4624–4632, 2011.
- 860 [22] F. Wang, W. Lin, Z. Ling, and X. Fang. A comprehensive review on phase change material emulsions: Fabrication, characteristics, and heat  
861 transfer performance. *Sol. Energy Mater Sol. Cells.*, 191:218–234, 2019.
- 862 [23] J. Shao, J. Darkwa, and G. Kokogiannakis. Review of phase change emulsions (pcmes) and their applications in hvac systems. *Energy and*  
863 *build.*, 94:200–217, 2015.
- 864 [24] L. Huang, M. Petermann, and C. Doetsch. Evaluation of paraffin/water emulsion as a phase change slurry for cooling applications. *Energy*,  
865 34(9):1145–1155, 2009.
- 866 [25] Q. Li, L. Fischer, G. Qiao, E. Mura, C. Li, and Y. Ding. High performance cooling of a hvdc converter using a fatty acid ester-based phase  
867 change dispersion in a heat sink with double-layer oblique-crossed ribs. *Int. J. Energy Res.*, 44(7):5819–5840, 2020.
- 868 [26] L. Fischer, E. Mura, P. O'Neill, S. von Arx, J. Worlitschek, G. Qiao, Q. Li, and Y. Ding. Thermophysical properties of a phase change  
869 dispersion for cooling around 50 C. *Int J Refrig.*, 119:410–419, 2020.
- 870 [27] B. Chen, X. Wang, Y. Zhang, H. Xu, and R. Yang. Experimental research on laminar flow performance of phase change emulsion. *Appl.*  
871 *Therm. Eng.*, 26(11-12):1238–1245, 2006.
- 872 [28] P. Schalbart, M. Kawaji, and K. Fumoto. Formation of tetradecane nanoemulsion by low-energy emulsification methods. *Int. J. Refrig.*,  
873 33(8):1612–1624, 2010.
- 874 [29] L. Huang, C. Doetsch, and C. Pollerberg. Low temperature paraffin phase change emulsions. *Int. J. Refrig.*, 33(8):1583–1589, 2010.
- 875 [30] W. Lu and S.A. Tassou. Experimental study of the thermal characteristics of phase change slurries for active cooling. *Appl. Energy*, 91(1):366–  
876 374, 2012.
- 877 [31] J. Shao, J. Darkwa, and G. Kokogiannakis. Development of a novel phase change material emulsion for cooling systems. *Renew. Energy*,  
878 87:509–516, 2016.
- 879 [32] L. Huang, P. Noeres, M. Petermann, and C. Doetsch. Experimental study on heat capacity of paraffin/water phase change emulsion. *Energy*  
880 *Convers. Manag.*, 51(6):1264–1269, 2010.
- 881 [33] L. Huang and M. Petermann. An experimental study on rheological behaviors of paraffin/water phase change emulsion. *Int. J. Heat Mass*



- 882 *Transf.*, 83:479–486, 2015.
- 883 [34] F. Wang, C. Zhang, J. Liu, X. Fang, and Z. Zhang. Highly stable graphite nanoparticle-dispersed phase change emulsions with little super-  
884 cooling and high thermal conductivity for cold energy storage. *Appl. Energy*, 188:97–106, 2017.
- 885 [35] F. Ma, J. Chen, and P. Zhang. Experimental study of the hydraulic and thermal performances of nano-sized phase change emulsion in horizontal  
886 mini-tubes. *Energy*, 149:944–953, 2018.
- 887 [36] E. Günther, T. Schmid, H. Mehling, S. Hiebler, and L. Huang. Subcooling in hexadecane emulsions. *Int J Refrig*, 33(8):1605–1611, 2010.  
888 Phase Change Materials and Slurries for Refrigeration and Air Conditioning.
- 889 [37] T. Morimoto, K. Suzuki, and H. Kumano. Heat transfer characteristics of phase change emulsions with solidification of phase change material  
890 particles in a circular tube. *Int. J. Refrig.*, 114:1–9, 2020.
- 891 [38] X. Zhang, J. Niu, and J. Wu. Evaluation and manipulation of the key emulsification factors toward highly stable pcm-water nano-emulsions  
892 for thermal energy storage. *Sol. Energy Mater Sol. Cells*, 219:110820, 2021.
- 893 [39] S. Abedi, N. Suteria, C. Chen, and S. Vanapalli. Microfluidic production of size-tunable hexadecane-in-water emulsions: Effect of droplet  
894 size on destabilization of two-dimensional emulsions due to partial coalescence. *J. Colloid Interface Sci.*, 533:59–70, 2019.
- 895 [40] x. Zhang, J. Niu, S. Zhang, and J. Wu. PCM in water emulsions: Supercooling reduction effects of nano-additives, viscosity effects of  
896 surfactants and stability. *Adv. Eng. Mater.*, 17(2):181–188, 2015.
- 897 [41] X. Zhang, J. Niu, and J. Wu. Development and characterization of novel and stable silicon nanoparticles-embedded pcm-in-water emulsions  
898 for thermal energy storage. *Appl. Energy*, 238:1407–1416, 2019.
- 899 [42] D. Cabaleiro, F. Agresti, S. Barison, M. Marcos, J. Prado, S. Rossi, S. Bobbo, and L. Fedele. Development of paraffinic phase change material  
900 nanoemulsions for thermal energy storage and transport in low-temperature applications. *Appl. Therm. Eng.*, 159:113868, 2019.
- 901 [43] G. Hagelestein and S. Gschwander. Reduction of supercooling in paraffin phase change slurry by polyvinyl alcohol. *Int. J. Refrig.*, 84:67–75,  
902 2017.
- 903 [44] C. Ho, C. Lee, and M. Yamada. Experiments on laminar cooling characteristics of a phase change nanofluid flow through an iso-flux heated  
904 circular tube. *Int. J. Heat Mass Transf.*, 118:1307–1315, 2018.
- 905 [45] S. Puupponen, A. Seppälä, O. Vartia, K. Saari, and T. Ala-Nissilä. Preparation of paraffin and fatty acid phase changing nanoemulsions for  
906 heat transfer. *Thermochimica Acta*, 601:33–38, 2015.
- 907 [46] B. Sivapalan, M. Neelesh Chandran, S. Manikandan, M. Saranprabhu, S. Pavithra, and K. Rajan. Paraffin wax–water nanoemulsion: A superior  
908 thermal energy storage medium providing higher rate of thermal energy storage per unit heat exchanger volume than water and paraffin wax.  
909 *Energy Convers. Manag.*, 162:109–117, 2018.
- 910 [47] K. Golemanov, S. Tcholakova, N. Denkov, and T. Gurkov. Selection of surfactants for stable paraffin-in-water dispersions, undergoing solidliq-  
911 uid transition of the dispersed particles. *Langmuir*, 22(8):3560–3569, 2006.
- 912 [48] T. Kousksou, T. El Rhafiki, M. Mahdaoui, P. Bruel, and Y. Zeraoui. Crystallization of supercooled pcms inside emulsions: Dsc applications.  
913 *Sol. Energy Mater Sol. Cells*, 107:28–36, 2012.
- 914 [49] S. Saarinen, S. Puupponen, A. Meriläinen, A. Joneidi, A. Seppälä and K. Saari, and T. Ala-Nissila. Turbulent heat transfer characteristics  
915 in a circular tube and thermal properties of n-decane-in-water nanoemulsion fluids and micelles-in-water fluids. *Int. J. Heat Mass Transf.*,  
916 81:246–251, 2015.
- 917 [50] V. Vasile, H. Necula, A. Badea, R. Revellin, J. Bonjour Jocelyn, and P. Haberschill. Experimental study of the heat transfer characteristics of  
918 a paraffin-in-water emulsion used as a secondary refrigerant. *Int. J. Refrig.*, 88:1–7, 2018.
- 919 [51] R. Yang, H. Xu, and Y. Zhang. Preparation, physical property and thermal physical property of phase change microcapsule slurry and phase  
920 change emulsion. *Sol. Energy Mater Sol. Cells*, 80(4):405–416, 2003.
- 921 [52] L. Royon, P. Perrot, G. Guiffant, and S. Fraoua. Physical properties and thermorheological behaviour of a dispersion having cold latent heat  
922 storage material. *Energy conversion and management*, 39(15):1529–1535, 1998.
- 923 [53] C. Eunsoo, Y. Cho, and H. Lorsch. Forced convection heat transfer with phase-change-material slurries: turbulent flow in a circular tube. *Int.*  
924 *J. Heat Mass Transf.*, 37(2):207–215, 1994.
- 925 [54] L. Fischer, S. Maranda, A. Stamatou, S. von Arx, and J. Worlitschek. Experimental investigation on heat transfer with a phase change  
926 dispersion. *Appl. Therm. Eng.*, 147:61–73, 2019.
- 927 [55] R. Ravotti, O. Fellmann, N. Lardon, L. Fischer, A. Stamatou, and J. Worlitschek. Synthesis and investigation of thermal properties of highly  
928 pure carboxylic fatty esters to be used as PCM. *Appl. Sci.*, 8(7):1069, Jun 2018.
- 929 [56] L. Fischer, A. Stamatou, S. von Arx, M. Pfister, S. Züst, and J. Worlitschek. Investigation of heat transfer in phase change dispersions (PCD).  
930 *JP Journal of Heat and Mass Transfer.*, 14(4):485–510, 2017.
- 931 [57] S. Nižetić, M. Jurčević, M. Arici, A. Arasu, and G. Xie. Nano-enhanced phase change materials and fluids in energy applications: A review.  
932 *Renew. Sust. Energ. Rev.*, 129:109931, 2020.
- 933 [58] F. Wang, W. Lin, Z. Ling, and X. Fang. A comprehensive review on phase change material emulsions: Fabrication, characteristics, and heat  
934 transfer performance. *Sol. Energy Mater Sol. Cells*, 191:218–234, 2019.
- 935 [59] D. Zou, Z. Feng, R. Xiao, K. Qin, J. Zhang, W. Song, and Q. Tu. Preparation and flow characteristic of a novel phase change fluid for latent  
936 heat transfer. *Sol. Energy Mater Sol. Cells*, 94(12):2292–2297, 2010.
- 937 [60] Y. Tokiwa, H. Sakamoto, T. Takiue, M. Aratono, H. Matsubara, and C. Bain. Effect of surface freezing on stability of oil-in-water emulsions.  
938 *Langmuir.*, 34(21):6205–6209, 2018.
- 939 [61] L. Orafidiya and F. Oladimeji. Determination of the required hlb values of some essential oils. *Int. J. Pharm.*, 237(1):241–249, 2002.
- 940 [62] H. Xu, R. Yang, Y. Zhang, Z. Huang, J. Lin, and X. Wang. Thermal physical properties and key influence factors of phase change emulsion.  
941 *Chinese Sci. Bull.*, 50(1):88–93, 2005.
- 942 [63] A. Wiącek and E. Chibowski. Zeta potential, effective diameter and multimodal size distribution in oil/water emulsion. *Colloid. Surf. A:*  
943 *Physiochem. Eng. Asp.*, 159(2):253–261, 1999.
- 944 [64] D. Cabaleiro, S. Hamze, F. Agresti, P. Estellé, S. Barison, L. Fedele, and S. Bobbo. Dynamic viscosity, surface tension and wetting behavior

- 945 studies of paraffin-in-water nano-emulsions. *Energies*, 12(17), 2019.
- 946 [65] A. Jadhav, C. Holkar, S. Karekar, D. Pinjari, and A. Pandit. Ultrasound assisted manufacturing of paraffin wax nanoemulsions: Process  
947 optimization. *Ultrasonics Sonochemistry*, 23:201–207, 2015.
- 948 [66] Y. Wu, M. Alivand, G. Hu, G. Stevens, and K. Mumford. Nucleation kinetics of glycine promoted concentrated potassium carbonate solvents  
949 for carbon dioxide absorption. *Chem. Eng. J.*, 381:122712, 2020.
- 950 [67] J. Coupland. Crystallization of lipids in oil-in-water emulsion states. *Crystallization of lipids: Fundamentals and applications in food,  
951 cosmetics, and pharmaceuticals*, page 431, 2018.
- 952 [68] T. El Rhafiki, T. Kousksou, A. Jamiland S. Jegadheeswaran, S. Pohekar, and Y. Zeraoui. Crystallization of pcms inside an emulsion: Super-  
953 cooling phenomenon. *Sol. Energy Mater Sol. Cells*, 95(9):2588–2597, 2011.
- 954 [69] G. Höhne, W. Hemminger, and H. Flammersheim. *Differential scanning calorimetry*. Springer Science & Business Media, 2013.
- 955 [70] W. Yu, D. France, E. Timofeeva, D. Singh, and J. Routbort. Comparative review of turbulent heat transfer of nanofluids. *Int. J. Heat Mass  
956 Transf.*, 55(21-22):5380–5396, 2012.
- 957 [71] F. Liu, Q. Chen, Z. Kang, W. Pan, D. Zhang, and L. Wang. Non-fourier heat conduction in oil-in-water emulsions. *Int. J. Heat Mass Transf.*,  
958 135:323–330, 2019.
- 959 [72] C. Ho and J. Gao. Preparation and thermophysical properties of nanoparticle-in-paraffin emulsion as phase change material. *Int. Commun.  
960 Heat Mass.*, 36(5):467–470, 2009.
- 961 [73] J. Maxwell. Electricity and magnetism. *Clarendon Press, Oxford, UK*, 1873.
- 962 [74] R. Hamilton and O. Crosser. Thermal conductivity of heterogeneous two-component systems. *Ind. Eng. Chem.*, 1(3):187–191, 1962.
- 963 [75] Z. Kang, P. Zhu, D. Gui, and L. Wang. A method for predicting thermal waves in dual-phase-lag heat conduction. *Int. J. Heat Mass Transf.*,  
964 115:250–257, 2017.
- 965 [76] M. Delgado, A. Lázaro, J. Mazo, C. Peñalosa, P. Dolado, and B. Zalba. Experimental analysis of a low cost phase change material emulsion  
966 for its use as thermal storage system. *Energy Convers. Manag.*, 106:201–212, 2015.
- 967 [77] H. Inaba and S. Morita. Flow and cold heat-storage characteristics of phase-change emulsion in a coiled double-tube heat exchanger. *J. Heat  
968 Trans.*, 117:440, 1995.
- 969 [78] Z. Zhao and Y. Shi. Experimental investigations of flow resistance and convection heat transfer and prediction of cold heat-storage character-  
970 istics for a phase-change emulsion in a coiled circular tube. *Heat Transf. Eng.*, 26(6):32–44, 2005.
- 971 [79] F. Ostwald. The theory of solutions. *Z. Phys. Chem.*, 2:36–37, 1888.
- 972 [80] H. Inaba, C. Dai, and A. Horibe. Natural convection heat transfer of microemulsion phase-change-material slurry in rectangular cavities heated  
973 from below and cooled from above. *Int. J. Heat Mass Transf.*, 46(23):4427–4438, 2003.
- 974 [81] M. Takashi and Hiroyuki K. Flow and heat transfer characteristics of phase change emulsions in a circular tube: Part 2. turbulent flow. *Int. J.  
975 Heat Mass Transf.*, 117:903–911, 2018.
- 976 [82] S. Roy and B. Avanic. Laminar forced convection heat transfer with phase change material suspensions. *Int. Commun. Heat Mass Transf.*,  
977 28(7):895–904, 2001.
- 978 [83] Y. Cho, E. Choi, and H. Lorsch. A novel concept for heat transfer fluids used in district cooling systems. Technical report, Drexel Univ.,  
979 Philadelphia, PA (United States). Dept. of Mechanical ..., 1991.
- 980 [84] D. Wen and Y. Ding. Experimental investigation into convective heat transfer of nanofluids at the entrance region under laminar flow conditions.  
981 *Int. J. Heat Mass Transf.*, 47(24):5181–5188, 2004.
- 982 [85] J. Bonjour, R. Revellin, P. Haberschill, V. Vasile, A. Badea, and H. Nacula. Theoretical evaluation of the use of phase change material  
983 emulsions and figures of merit. In *2019 International Conference on ENERGY and ENVIRONMENT (CIEM)*, pages 520–523. IEEE, 2019.
- 984 [86] J. Ho, N. Wijeyesundera, S. Rajasekar, and T. Chandratilleke. Performance of a compact, spiral coil heat exchanger. *Heat Recovery Systems  
985 and CHP*, 15(5):457–468, 1995.
- 986 [87] S. Memon, M. Sajid, M. Malik, A. Alquaity, M. Rehman, T. Cheema, M. Kwak, and C. Park. Investigation of the thermal performance of salt  
987 hydrate phase change of nanoparticle slurry flow in a microchannel. *J. Chem.*, 2019.
- 988 [88] L. Yeh, R. Chu, and W. Janna. Thermal management of microelectronic equipment: Heat transfer theory, analysis methods, and design  
989 practices. asme press book series on electronic packaging. *Appl. Mech. Rev.*, 56(3):B46–B48, 2003.
- 990 [89] R. Prasher, D. Song, and J. Wang. Measurements of nanofluid viscosity and its implications for thermal applications. *Appl. Phys. Lett.*,  
991 89:133108, 2006.